Published for SISSA by Springer

Received: July 6, 2017
Revised: September 29, 2017
Accepted: October 8, 2017
Published: October 19, 2017

Search for top quark decays $t \to qH$, with $H \to \gamma\gamma$, in $\sqrt{s} = 13$ TeV pp collisions using the ATLAS detector

The ATLAS collaboration

E-mail: atlas.publications@cern.ch

Abstract: This article presents a search for flavour-changing neutral currents in the decay of a top quark into an up-type ($q = c, u$) quark and a Higgs boson, where the Higgs boson decays into two photons. The proton-proton collision data set analysed amounts to 36.1 fb^{-1} at $\sqrt{s} = 13$ TeV collected by the ATLAS experiment at the LHC. Top quark pair events are searched for, where one top quark decays into qH and the other decays into bW. Both the hadronic and leptonic decay modes of the W boson are used. No significant excess is observed and an upper limit is set on the $t \to cH$ branching ratio of 2.2×10^{-3} at the 95% confidence level, while the expected limit in the absence of signal is 1.6×10^{-3}. The corresponding limit on the tcH coupling is 0.090 at the 95% confidence level. The observed upper limit on the $t \to uH$ branching ratio is 2.4×10^{-3}.

Keywords: Flavour Changing Neutral Currents, Hadron-Hadron scattering (experiments), Higgs physics, Top physics

ArXiv ePrint: 1707.01404

https://doi.org/10.1007/JHEP10(2017)129

Contents

JHEP10(2017)129

1 Introduction

The discovery of the Higgs boson in 2012, by the ATLAS and CMS collaborations [1, 2], has opened the possibility of searching, among the abundant $t\bar{t}$ final states produced in proton-proton collisions at the CERN Large Hadron Collider (LHC), for the decay $t \to qH$ of a top quark (or antiquark) into an on-shell Higgs boson, of mass 125.09 GeV [3], plus an up-type quark (or antiquark), $q = c$ or u. This decay, which proceeds via a flavour-changing neutral current (FCNC), is forbidden at tree level in the Standard Model (SM) and, with respect to the dominant top quark decay mode ($t \to bW$), is suppressed at higher orders due to the Glashow-Iliopoulos-Maiani mechanism [4]. The $t \to qH$ branching ratio ($\mathcal{B}$) in the SM is estimated to be around 3×10^{-15} (see ref. [5] and references therein), and an observation of this decay would provide a clear signal of physics beyond the SM (BSM).

In BSM models, different mechanisms can yield effective couplings orders of magnitude larger than those of the SM. Examples of such extensions are the quark-singlet model [6–8], the two-Higgs-doublet model with or without flavour violation [9–17], the minimal supersymmetric standard model [18–24], Supersymmetry with R-parity violation [25], the Topcolour-assisted Technicolour model [26], models with warped extra dimensions [27–29] and the Littlest Higgs model with T-parity conservation [30]. In composite Higgs boson models, FCNC may appear even with a single Higgs doublet [29], inducing $t \to cH$ branching ratios up to 10^{-4}. For a recent review, see ref. [31].

Among all the possibilities, the largest branching ratio $\mathcal{B} \sim 1.5 \times 10^{-3}$ appears in the ansatz of Cheng and Sher [9] in which the tree-level coupling remains allowed in the absence of an additional symmetry, and scales with the top and up-type quark masses, m_t and m_q, as $\lambda_{tqH} = \sqrt{2m_q m_t}/v$ (where $v = 246\,\text{GeV}$ is the Higgs field vacuum expectation value). This can be regarded as the "maximal naturalness" approach in the Higgs flavour structure.

In this article, the $t \to qH$ decay is searched for using $36.1\,\text{fb}^{-1}$ of 13 TeV proton-proton collision data taken in 2015 and 2016 with the ATLAS detector at the LHC. The search uses the $H \to \gamma\gamma$ decay mode, taking advantage of the clean diphoton signature, despite its small branching ratio (0.23% in the SM [32]).

A search for $t \to qH$ decays was previously performed at $\sqrt{s} = 7$ and 8 TeV with Run-1 data, both in ATLAS and in CMS. As the $t \to cH$ and $t \to uH$ modes are hard to distinguish, the upper limits are given assuming that each final state is produced alone. In ATLAS, the $H \to \gamma\gamma$ channel [33] yields the observed and expected limits on $\mathcal{B}(t \to cH)$ of 0.79% and 0.51% respectively, at the 95% confidence level (CL). Combining with the multi-lepton[1] and $H \to b\bar{b}$ final states, which, at 8 TeV, are each comparable in sensitivity to the $H \to \gamma\gamma$ channel, the overall observed (expected) limit at the 95% CL is 0.46% (0.25%) for $t \to cH$ and 0.45% (0.29%) for $t \to uH$ [34]. The 95% CL observed (expected) limits from the CMS Collaboration on the $t \to cH$ and $t \to uH$ branching ratios are 0.40% (0.43%) and 0.55% (0.40%) respectively [35], using the same final states as ATLAS.

Compared to the previous ATLAS result in the $H \to \gamma\gamma$ mode, a significant improvement is attained due to the large increase (about four times) in the $t\bar{t}$ production cross section when increasing the centre-of-mass energy from 8 TeV to 13 TeV, and the larger integrated luminosity recorded during 2015 and 2016. Adverse effects are the increase in the production cross section of backgrounds, and the significantly larger "pile-up" noise due to the superimposition of additional interactions on the selected hard interaction.

The analysis aims to select $t\bar{t}$ pairs with one top quark decaying into bW (SM decay) and the other into qH. It is split into two final states, targeting the decay of the W boson from the SM top quark decay either in the hadronic mode (hadronic selection) or in the leptonic mode (leptonic selection). The result is extracted from a fit to the diphoton invariant mass spectra of a resonant signal function centred around the Higgs boson mass and a background function, mainly constrained by bands on either side of the signal regions. While this data driven approach does not require a detailed understanding of the background, the dominant contributions are however presented together with the data, at different stages of the analysis.

[1]The multi-lepton final state includes events from the $H \to ZZ^*, WW^*$ and $\tau^+\tau^-$ decays.

JHEP10(2017)129

In this analysis, SM production of the Higgs boson, with its subsequent decay into a diphoton final state, is considered as a background, described by the same diphoton invariant mass distribution as the sought-for FCNC production. Its magnitude, determined by simulation, is accounted for in the signal extraction.

2 Detector, data set and simulation samples

2.1 ATLAS detector

The ATLAS detector [36] consists of an inner detector for tracking surrounded by a superconducting solenoid providing a 2 T magnetic field, electromagnetic and hadronic calorimeters, and a muon spectrometer. The inner detector provides tracking in the pseudorapidity[2] region $|\eta| < 2.5$ and consists of silicon pixel and microstrip detectors inside a transition radiation tracker that covers $|\eta| < 2.0$. A new innermost silicon pixel layer has been added to the inner detector after the Run-1 data taking [37, 38]. The electromagnetic calorimeter, a lead/liquid-argon sampling device with accordion geometry, is divided into one barrel ($|\eta| < 1.475$) and two end-cap ($1.375 < |\eta| < 3.2$) sections. Longitudinally, it is divided into three layers. While most of the energy is deposited in the second layer, the first layer, referred to as the strip layer, has fine segmentation in the regions $|\eta| < 1.4$ and $1.5 < |\eta| < 2.4$ to facilitate the separation of photons from neutral hadrons and to allow shower directions to be measured. In the range of $|\eta| < 1.8$, a presampler layer allows the energy to be corrected for losses upstream of the calorimeter. The barrel ($|\eta| < 1.7$) hadronic calorimeter consists of steel and scintillator tiles, while the end-cap sections ($1.5 < |\eta| < 3.2$) are composed of copper and liquid argon. The forward calorimeter ($3.1 < |\eta| < 4.9$) uses copper and tungsten as absorber with liquid argon as active material. The muon spectrometer consists of precision ($|\eta| < 2.7$) and trigger ($|\eta| < 2.4$) chambers equipping a toroidal magnet system which surrounds the hadronic calorimeter.

2.2 Data set

This analysis uses the full proton-proton data set recorded by ATLAS in 2015 and 2016 with the LHC operating at a centre-of-mass energy $\sqrt{s} = 13\,\text{TeV}$ and a bunch spacing of 25 ns. After application of data-quality requirements, the integrated luminosity amounts to $36.1\,\text{fb}^{-1}$, with a relative uncertainty of 3.2%.[3] The data were recorded with instantaneous luminosities up to $1.4\times10^{34}\,\text{cm}^{-2}\text{s}^{-1}$. The mean number of interactions per bunch crossing, μ, was on average 13 in 2015 and 25 in 2016. The inelastic collisions that occur in addition

[2] ATLAS uses a right-handed coordinate system with its origin at the nominal interaction point (IP) in the centre of the detector and the z-axis along the beam line. Observables labelled as transverse are projected onto the x–y plane. The x-axis points from the IP to the centre of the LHC ring, and the y-axis points upwards. Cylindrical coordinates (r, ϕ) are used in the transverse plane, ϕ being the azimuthal angle around the beam line. The pseudorapidity is defined in terms of the polar angle θ as $\eta = -\ln\tan(\theta/2)$. The angular distance ΔR is defined as $\Delta R \equiv \sqrt{(\Delta\eta)^2 + (\Delta\phi)^2}$. The transverse energy is $E_{\text{T}} = E/\cosh(\eta)$.

[3] The uncertainty is derived, following a methodology similar to that detailed in ref. [39], from a preliminary calibration of the luminosity scale using x–y beam-separation scans performed in August 2015 and May 2016.

JHEP10(2017)129

to the hard interaction produce mainly low transverse momentum particles that form the pile-up background.

The data considered here were selected using a diphoton trigger which requires two clusters formed from energy deposits in the electromagnetic calorimeter. The transverse energy threshold was 35 GeV (25 GeV) for the leading (sub-leading) cluster (sorted in E_{T}). Loose criteria were applied to ensure that the shape of selected clusters matched that expected for electromagnetic showers initiated by photons. The efficiency of the trigger for events containing two photons passing the offline selection requirements of this analysis was measured to be larger than 99%.

2.3 Signal and background simulation

The FCNC signal was simulated using MG5_aMC@NLO 2.4.3 [40] interfaced to Pythia 8.212 [41] with the `A14` [42] set of tuned parameters for the modelling of parton showers, hadronisation and multiple interactions. The $t\bar{t}$ pairs were generated at next-to-leading order (NLO) in quantum chromodynamics (QCD) with the TopFCNC UFO model [43], using the 5-flavour scheme and the NNPDF3.0 [44] parton distribution functions (PDFs). The factorisation and renormalisation scales were set equal to $\sqrt{m_t^2 + (p_{\mathrm{T},t}^2 + p_{\mathrm{T},\bar{t}}^2)/2}$, where $p_{\mathrm{T},t}$ ($p_{\mathrm{T},\bar{t}}$) is the transverse momentum of the top quark (antiquark). The top quark decay was performed by MadSpin, and the Higgs boson decay by Pythia 8. Two samples corresponding to $t\bar{t}$ production with one top quark decaying into a charm quark and a Higgs boson (which itself decays into two photons with 100% branching ratio) were produced. The two samples, added together, correspond to the W bosons from $t \to bW$ decaying leptonically or hadronically. The leptonic decays of the W include all three lepton flavours. The top quark mass taken in the simulation is 172.5 GeV, and the Higgs boson mass is 125 GeV. Two equivalent samples with $t \to uH$ were also produced. The $t\bar{t}$ cross section used is 832^{+40}_{-46} pb. It has been calculated at next-to-next-to leading order in QCD including resummation of next-to-next-to-leading logarithmic soft gluon terms with Top++2.0 [45, 46].

The contribution from known production sources of Higgs bosons, followed by a decay into two photons, is considered here as a resonant background. The following production modes, ordered by their cross sections, were considered and simulated [47]: gluon-gluon fusion (ggH), vector-boson fusion (VBF) and associated production (WH, ZH, $t\bar{t}H$, $b\bar{b}H$, $tHjb$, and tWH). The Higgs boson cross sections and branching ratios compiled by the LHC Higgs Cross-Section Working Group [32] are used for normalisation. For ggH, the QCD next-to-next-to-next-to-leading-order cross section is used. For tWH, the NLO normalisation given in ref. [48] is used.

The ggH and VBF events were generated at NLO using Powheg [49, 50] interfaced to Pythia 8 with the `AZNLO` [51] set of tuned parameters for parton showering, hadronisation and multiple interactions. The events from WH and ZH associated production were generated at leading order with Pythia 8. Associated $t\bar{t}H$ production was generated at NLO with MG5_aMC@NLO interfaced with Pythia 8. The parton distribution functions CT10 [52], NNPDF3.0 and CTEQ6L1 [53] were used for the Powheg, MG5_aMC@NLO and Pythia 8 samples, respectively.

JHEP10(2017)129

An event sample corresponding to non-resonant diphoton production, labelled $S_{\gamma\gamma j}$ in the following, was generated with the Sherpa 2.1.1 event generator [54], with up to three additional partons in the matrix element. This sample is used as a benchmark sample for non-resonant background production.

Samples of events from $t\bar{t}$, W and Z production with one or two photons generated in the matrix element were also simulated. Due to initial-state radiation (ISR), final-state radiation (FSR) and jets faking photons, the one- and two-photon samples partly overlap, the first one including an approximation of the second one. Given the cross sections of the simulated processes, and the statistical size of the available samples, the $t\bar{t}\gamma$, $W\gamma\gamma$ and $Z\gamma\gamma$ samples were selected to represent each of the backgrounds, albeit with a large uncertainty in the corresponding cross sections.

The stable particles, defined as particles with a lifetime longer than 10 ps, were passed through a full detector simulation [55] based on Geant4 [56]. The resulting "particle hits" in the active detector material were subsequently transformed into detector signals during digitisation.

Pile-up was modelled using simulated minimum-bias events generated using Pythia 8. The number of events overlaid onto the hard-scattering events during the digitisation was randomly chosen so as to reproduce the distribution of μ observed in data. The effects from pile-up events occurring in nearby bunch crossings (out-of-time pile-up) were also modelled.

3 Event reconstruction and candidate selection

3.1 Event reconstruction

While the requirement of two tightly identified and precisely measured photons is the key part of the selection, the analysis also requires jets and b-tagging for the hadronic selection as well as identified electrons or muons and missing transverse momentum (with magnitude $E_{\mathrm{T}}^{\mathrm{miss}}$) for the leptonic selection. A minimum angular distance (ΔR) is required between these objects. If some objects overlap after reconstruction, a removal is performed, keeping, in order of priority, photons, then leptons, and finally jets.

The photon reconstruction [57] is seeded by clusters of energy deposits in the electromagnetic calorimeter with transverse energy greater than 2.5 GeV in a region of 0.075×0.125 in $\eta\times\phi$. The accepted $|\eta|$ region extends from 0 up to 2.37 excluding the region [1.37, 1.52], which is less instrumented and where dead material affects both the identification and the energy measurement. The reconstruction is designed to separate electrons from unconverted and converted photons. Clusters without any matching track or conversion vertex are classified as unconverted photon candidates while clusters with a matching conversion vertex are classified as converted photon candidates. In simulation, when requiring the generated photon E_{T} to be above 20 GeV, the reconstruction efficiency is 98% on average for converted and unconverted photons.

The photon energy is measured from clusters of size 0.075×0.175 in $\eta\times\phi$ in the barrel region of the calorimeter and 0.125×0.125 in the calorimeter end-caps, using a combination of simulation-based and data-driven calibration factors [58] determined from $Z\to e^+e^-$

JHEP10(2017)129

events collected in 2015 and 2016. The photon energy resolution in simulation is corrected to match the resolution in data [59].

The identification of photons [57] is based on lateral and longitudinal shower shapes measured in the electromagnetic calorimeter. Two working points, "loose" and "tight", are defined. Photon candidates are required to deposit only a small fraction of their energy in the hadronic calorimeter and to have a lateral shower shape consistent with that expected from a single electromagnetic shower. The information about the shape of the shower from the highly segmented strip layer of the calorimeter is used to discriminate single photons from hadronic jets in which a neutral meson carries most of the jet energy. The "tight" identification efficiency, averaged over η, for unconverted (converted) photons ranges from 85% to 95% (90% to 98%) for E_{T} between 25 GeV and 200 GeV [60].

To suppress the hadronic background, the photon candidates are required to be isolated from any other significant activity in the calorimeter and the tracking detectors. The calorimeter isolation is computed as the sum of the transverse energy of positive-energy topological clusters[4] reconstructed in a cone of $\Delta R = 0.2$ around the photon candidate. The transverse energy of the photon candidate is subtracted from the sum. The contributions of underlying event and pile-up are subtracted based on the method suggested in ref. [62]. The track isolation is computed as the scalar sum of the transverse momentum p_{T} of all tracks with $p_{\mathrm{T}} > 1$ GeV within a cone of $\Delta R = 0.2$ around the photon candidate. The tracks must satisfy some loose track quality criteria and originate from the interaction vertex (see below). For converted photon candidates, the tracks associated with the conversion are removed. For the "loose" isolation working point chosen in this analysis, the calorimeter (track) isolation is required to be less than 6.5% (5%) of the photon transverse energy. The efficiency of the calorimeter isolation requirement ranges from 83% to 97% for photons of E_{T} between 25 GeV and 200 GeV which pass the identification requirements. The efficiency of the track isolation requirement ranges from 96% to 100% (93% to 97%) for unconverted (converted) photons of E_{T} between 25 GeV and 200 GeV which pass the identification and calorimeter isolation requirements. A dedicated study using electrons and positrons from Z boson decays as a proxy for photons showed that the ratio of isolation efficiencies in data and simulation remains constant at 1.01 ± 0.01 per event, for events with up to four reconstructed jets.

The identification of the interaction vertex uses a neural network algorithm based on tracks and primary vertex information, as well as on the two photon directions measured in the calorimeter and inner detector (in the case of a conversion) [63]. Given the presence of jets in the selected sample, the vertex identification efficiency is high, with 97% of selected vertices falling within $\pm$ 1 mm of the true position, for events with four or more reconstructed jets.

Jets are reconstructed from topological clusters using the anti-k_t algorithm [64] with a radius parameter $R = 0.4$ and are required to have an $|\eta_{\mathrm{det}}| < 4.4$, where η_{det} is the jet pseudorapidity assuming the interaction point is at the nominal collision position. The

[4]Topological clusters are three-dimensional clusters of variable size, built by clustering calorimeter cells on the basis of the signal-to-noise ratio [61].

JHEP10(2017)129

dependence of the jet response on the number of primary vertices and the average number of interactions is mitigated by applying a data-driven event-by-event subtraction procedure based on the jet area [62]. In order to suppress jets produced in additional pile-up interactions, each jet with $|\eta| < 2.4$ and $p_{\mathrm{T}} < 60\,\mathrm{GeV}$ is required to have a "jet vertex tagger (JVT) parameter" value larger than 0.59 [65]. The corresponding efficiency for jets from the hard interaction, in a sample of simulated ggH events, with $H \to \gamma\gamma$, is estimated to be 86%, with a purity (fraction of jets originating from the hard interaction) of 90%. These fractions are significantly higher (94% and 99% respectively), for the sample of simulated $t\bar{t}H$ events, with $H \to \gamma\gamma$.

Jets containing b-hadrons are identified (b-tagged) using the MV2c10 tagger [66, 67], with a selection threshold corresponding to a 77% efficiency for jets containing a b-hadron in $t\bar{t}$ events. The corresponding rejection factor of jets originating from light quarks or gluons is ~ 130 and it is ~ 6 for charm quark jets.

Electron candidates consist of clusters of energy deposited in the electromagnetic calorimeter that are associated with tracks in the inner detector [68], and are consistent with those expected for electromagnetic showers. The electron transverse momentum is computed from the cluster energy and the track direction at the interaction point. Furthermore, all tracks associated with electromagnetic clusters are refitted using a Gaussian-sum Filter [69], which accounts for bremsstrahlung energy losses. Electron candidates are required to satisfy $E_{\mathrm{T}} > 15\,\mathrm{GeV}$ and $|\eta_{\mathrm{cl}}| < 2.47$, excluding $1.37 < |\eta_{\mathrm{cl}}| < 1.52$ (η_{cl} is the pseudorapidity of the electromagnetic cluster). In addition, the transverse impact parameter significance of the associated track must be below 5σ and the longitudinal impact parameter must fulfil $|z_0 \sin\theta| < 0.5$ mm. Electron candidates are required to be of "medium" quality [70], and to satisfy loose calorimeter and track isolation criteria with thresholds tuned to have an average efficiency of $\sim 98\%$.

Muons are required to meet the conditions $|\eta| < 2.7$ and $p_{\mathrm{T}} > 10\,\mathrm{GeV}$, and to be of "medium" quality [71]. The transverse impact parameter significance of the muon tracks must be below 3σ and the longitudinal impact parameter must fulfil $|z_0 \sin\theta| < 0.5$ mm. Muon candidates are required to satisfy track isolation [71] criteria with a p_{T} independent efficiency of 99%.

Missing transverse momentum is calculated as the negative vector sum of the transverse momentum of all objects in an event [72]. Jets not satisfying the JVT criterion or with $p_{\mathrm{T}} < 20\,\mathrm{GeV}$ are removed, but their associated tracks originating from the interaction vertex are included in a dedicated *soft term*.

The selection of candidate events starts by applying the "tight diphoton selection": at least two photons satisfying the "tight" identification criteria, with loose calorimeter and track isolation, $p_{\mathrm{T}} > 40\,\mathrm{GeV}$ ($p_{\mathrm{T}} > 30\,\mathrm{GeV}$) for the leading (sub-leading) photon candidate, and diphoton invariant mass between 100 GeV and 160 GeV. The number of events passing this requirement in data is about four hundred thousand. Events without identified leptons (electron or muon) enter the hadronic selection; those with exactly one lepton enter the leptonic selection. Events with two or more identified leptons are rejected.

JHEP10(2017)129

3.2 Hadronic selection

Jets passing the reconstruction and selection described in section 3.1 are used together with the two photons to select the final sample. The significance of the FCNC signal was optimised with $S/\sqrt{B}$ as figure of merit, where S and B are the numbers of events from the $t \to cH$ simulated signal sample and the $\mathrm{S}_{\gamma\gamma j}$ sample, respectively, both evaluated in the signal region (see below).

To reduce the contribution of pile-up jets, only jets with $p_{\mathrm{T}} > 30\,\mathrm{GeV}$ are considered. While in the background sample the distribution of the number of jets is a rapidly falling distribution, its counterpart for signal shows a broad peak around three to four. Events with at least four jets are kept for the hadronic analysis (about 9000 events remain at this stage), and only the four leading jets are used further in the analysis. In addition, it is required that at least one of the four jets is b-tagged.

The next step is designed to select events for which the six-body final state (two photons and four jets) is compatible with a $t\bar{t}$ final state. It starts by forming three-body objects: the two photons plus one jet on one side (Top1), and the three other jets on the other side (Top2). By grouping each of the four jets with the two photons, four (Top1,Top2) pairs are constructed, with corresponding invariant masses (M_1,M_2). For an event to be selected, there must be at least one combination (Top1,Top2) with masses (M_1,M_2) compatible with the top quark mass, as decribed below.[5]

The distributions of M_1 and M_2 are shown in figure 1; the M_1 distribution has four entries per event, while for M_2 only those combinations passing the M_1 selection, as described below, enter. In the signal distributions, the peaks from correctly reconstructed top quark decays are clearly visible, and particularly narrow in the Top1 distribution, while the combinatorial background has a shape similar to the distribution obtained with the $\mathrm{S}_{\gamma\gamma j}$ sample. The $\mathrm{S}_{\gamma\gamma j}$ sample is normalised to data, after subtraction of the $t\bar{t}\gamma$ contribution. The $W\gamma\gamma$ and $Z\gamma\gamma$ contributions are negligible.

Based on the position and width of the two signal peaks, the window chosen for the M_1 selection ranges from 152 GeV to 190 GeV, while for M_2 the broader range from 120 GeV to 220 GeV is chosen.

In order to increase the acceptance, albeit with a reduced signal-to-noise ratio, events failing the M_2 selection step are also retained for the final analysis by exploiting two (orthogonal) categories:

- category 1: events that pass the full selection;
- category 2: events that fail the M_2 requirement but satisfy all other selection criteria.

The category 1 (2) data sample has 115 (437) events. The corresponding acceptances for the simulated $t\bar{t}$ events with $t \to cH$ and $H \to \gamma\gamma$ are $(2.89 \pm 0.10)\%$ and $(4.15 \pm 0.12)\%$ for category 1 and 2 respectively, where the uncertainties are statistical only. During the optimisation phase of the analysis, the region between 122 GeV and 129 GeV where the

[5] An additional condition that the b-tagged jet belongs to Top2 was evaluated but not retained, as this slightly worsens the sensitivity for the $t \to cH$ mode, where the charm quark contributes to the overall b-tagging efficiency of an event.

JHEP10(2017)129

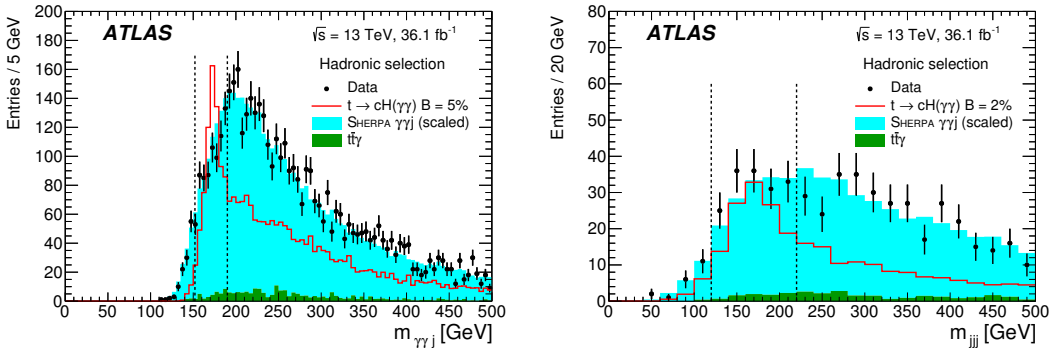

(a) **(b)**

Figure 1. Distribution of the invariant mass of (a) the two selected photons, together with one of the four selected jets (Top1, four entries per event), and (b) the three remaining jets (Top2, one entry per combination fulfilling the M_1 selection). At least one b-tagged jet per event is required. The $t\bar{t}\gamma$ distributions, normalised to the data's integrated luminosity using the theoretical cross section, are superimposed, together with the Sherpa $S_{\gamma\gamma j}$ contribution normalised to the difference between data and $t\bar{t}\gamma$. The signal distributions are normalised assuming a branching ratio of (a) 5% and (b) 2%. The vertical dotted lines indicate the (a) M_1 and (b) M_2 selection windows (see text).

sought-for FCNC signal is expected to appear, and called the signal region (SR) in the following, was masked (with a margin of 2 GeV on the low side and 1 GeV in the high side). The category 1 (2) data sample has 14 (69) events with the diphoton mass falling in the signal region.

The $\gamma\gamma$ invariant mass spectra for data and for the $S_{\gamma\gamma j}$ and $t\bar{t}\gamma$ samples are compared in figures 2(a) and 2(b) for categories 1 and 2, respectively. The normalisation of simulation to data excludes the mass range from 122 to 129 GeV in both cases. The $t\bar{t}\gamma$ contribution is normalised to the integrated luminosity of the data using its theoretical cross section, while $S_{\gamma\gamma j}$ covers the difference between data and $t\bar{t}\gamma$. The expected SM Higgs boson production and an additional FCNC signal normalised assuming $\mathcal{B} = 0.2\%$ are shown stacked over the sum of the backgrounds.

Good agreement is observed between the shapes of the data and the $\gamma\gamma$+jets background represented by the $S_{\gamma\gamma j}$ sample, for the M_1 and M_2 spectra shown in figure 1. Since this background and the data agree rather well in the sidebands of the $\gamma\gamma$ mass spectra (figure 2), the $S_{\gamma\gamma j}$ sample is used (see section 4) to determine the background fitting function needed for the final signal extraction.

3.3 Leptonic selection

The aim of the leptonic analysis is to identify $t\bar{t}$ events where one top quark decays into qH, and the W boson originating from the other top quark decays leptonically. Only electrons and muons are considered as candidates for lepton identification.

The selection of leptonic candidate events starts by applying the "tight diphoton selection". Requiring in addition one identified lepton reduces the sample to 833 events. The p_{T} threshold for leptons is set to 10 GeV for muons, and 15 GeV for electrons. The higher

JHEP10(2017)129

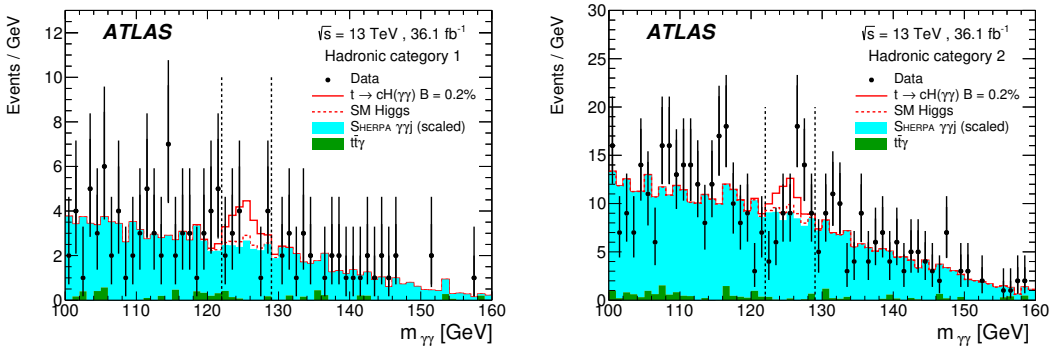

(a) **(b)**

Figure 2. Distributions of the diphoton invariant mass, for data events, the $t\bar{t}\gamma$ sample, and the $S_{\gamma\gamma j}$ sample for (a) category 1 and (b) category 2 of the hadronic selection. The $t\bar{t}\gamma$ sample is normalised using the data's integrated luminosity and the theoretical cross section. The SHERPA $S_{\gamma\gamma j}$ sample is normalised to the difference between data and $t\bar{t}\gamma$. The SM Higgs boson production and an additional FCNC signal normalised assuming $\mathcal{B} = 0.2\%$ are shown stacked over the sum of the backgrounds. The vertical dotted lines indicate the signal region (see text).

threshold in the electron case is motivated by a comparatively larger fraction of jets faking electrons. Requiring two or more jets with $p_{\mathrm{T}} > 30\,\mathrm{GeV}$ further reduces the sample to 223 events. Only the two leading jets are used further in the analysis.

The dominant background sources are $t\bar{t}\gamma$, $W\gamma\gamma$ and $Z\gamma\gamma$ and the diphoton + jets background, in which a small fraction of jets are wrongly identified as leptons.

In order to further select leptonic signal events, the missing transverse momentum is used to determine, with the lepton p_{T}, the transverse mass m_{T} whose distribution is shown in figure 3(a) for data and the relevant simulated samples. In the region between 56 GeV and 88 GeV the background prediction, dominated by $t\bar{t}\gamma$, $W\gamma\gamma$ and $Z\gamma\gamma$, significantly underestimates the data: while $25 \pm 3\%$ of data events fall in this region, the corresponding fraction for the simulation is $16 \pm 1\%$, where the uncertainties are statistical only. The discrepancy is attributed to the large uncertainty affecting the theoretical cross sections of these processes and to the lack of $W\gamma$ and $Z\gamma$ events with an extra photon from ISR, FSR or jets faking photons, for which the size of the simulated samples was not large enough to have a meaningful estimate after the full selection. Applying a scaling factor of 3 to the $W\gamma\gamma$ and $Z\gamma\gamma$ contributions (as derived from the comparison of the $t\bar{t}\gamma$ and $t\bar{t}\gamma\gamma$ samples), the fraction of simulated events with m_{T} between 56 GeV and 88 GeV becomes $27 \pm 1\%$, thus compatible with the data. As explained in section 1, the disagreement as observed in figure 3(a) does not affect the result because in the final fit (see section 4) the background is determined from data only. A selection requiring m_{T} larger than 30 GeV, which preserves a large fraction of the signal and rejects much of the background (especially from the $S_{\gamma\gamma j}$ sample), is applied. The number of data events remaining at this stage of the analysis is 124.

The next step is to verify, as was done for the hadronic selection, that the final-state particles are kinematically compatible with the decay of two top quarks. The invariant mass M_1 of the two photons and one of the two jets (Top1) is calculated, as well as the

JHEP10(2017)129

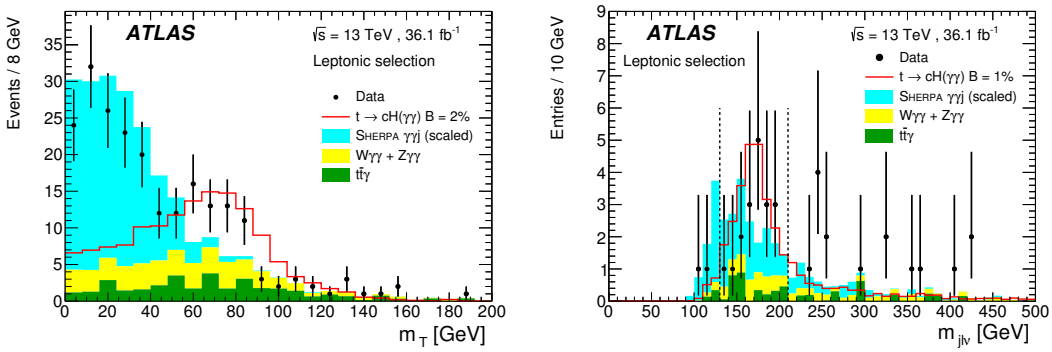

(a) **(b)**

Figure 3. Distribution (a) of the transverse mass calculated from the lepton kinematics and the missing transverse momentum and (b) of the invariant mass of the lepton, the neutrino, and one jet for each $\gamma\gamma j$ combination where the $m_{\gamma\gamma j}$ mass falls in the M_1 acceptance window. No b-tagging is required. The $t\bar{t}\gamma$, $W\gamma\gamma$ and $Z\gamma\gamma$ distributions are superimposed, normalised to the data's integrated luminosity using theoretical cross sections. The SHERPA $S_{\gamma\gamma j}$ sample is normalised to the difference between data and the sum of $t\bar{t}\gamma$, $W\gamma\gamma$ and $Z\gamma\gamma$. The distribution of the FCNC signal is normalised assuming a branching ratio of (a) 2% and (b) 1%. The vertical dotted lines in (b) indicate the M_2 selection window (see text).

mass M_2 of the remaining jet, the lepton, and the neutrino (Top2). For the latter, the neutrino longitudinal momentum is estimated by using a W boson mass constraint, as was done in ref. [33]. The same calculation is repeated, exchanging the role of the two jets. If the invariant masses (M_1, M_2) of one of the two (Top1, Top2) combinations fall in predefined windows around the top quark mass, the event is selected, provided one of the two jets is b-tagged. This defines category-1 events. Events fulfilling all requirements, except the one on M_2 are kept as category-2 events. As was done for the hadronic mode, the acceptance windows were optimised, resulting in the same interval for M_1 (152 GeV to 190 GeV), and in a slightly narrower interval for M_2, from 130 GeV to 210 GeV.

The event sample remaining at the end of the selection is extremely small. Three events are selected in each of category 1 and category 2. The corresponding acceptances for the simulated $t\bar{t}$ events with $t \to cH$ and $H \to \gamma\gamma$ are $(0.96 \pm 0.03)\%$ for category 1 and $(0.27 \pm 0.02)\%$ for category 2, where the uncertainties are statistical only. The corresponding diphoton invariant mass distributions are shown in figure 4. In this figure, the $t\bar{t}\gamma$, $W\gamma\gamma$ and $Z\gamma\gamma$ backgrounds, affected by large statistical fluctuations, are shown using large bins, 10 GeV wide. Only $t\bar{t}\gamma$ remains significant at this stage. Its contribution is normalised to the data's integrated luminosity using the theoretical cross section. Like for the hadronic analysis, the contributions from $S_{\gamma\gamma j}$ are normalised to match the number of events observed in the sidebands, once the $t\bar{t}\gamma$ background is taken into account. No contribution of this type is actually necessary for category 1. The expected SM Higgs boson contribution and an additional FCNC signal normalised assuming $\mathcal{B} = 0.2\%$ are shown stacked over the backgrounds.

JHEP10(2017)129

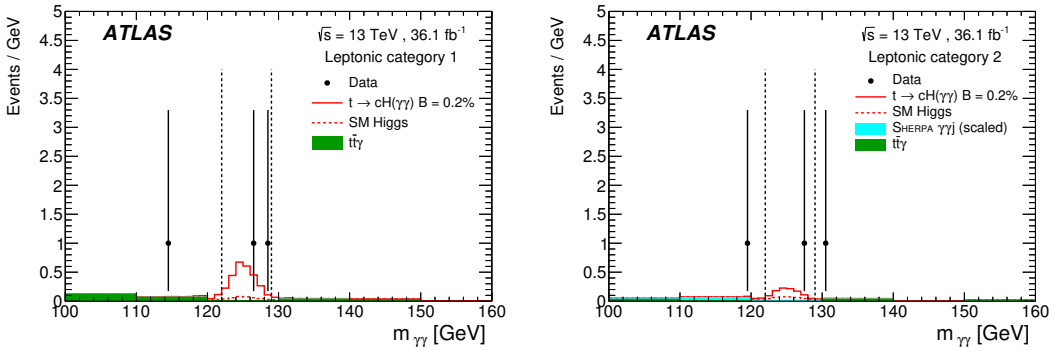

(a) **(b)**

Figure 4. Distributions of the diphoton invariant mass for (a) category 1 and (b) category 2 of the leptonic analysis. The $t\bar{t}\gamma$ distribution is normalised to the data's integrated luminosity using the theoretical cross section. The SHERPA $S_{\gamma\gamma j}$ contribution is shown for category 2, where its contribution is significant (see text). The SM Higgs boson production and an additional FCNC signal normalised assuming $\mathcal{B} = 0.2\%$ are shown stacked over the backgrounds. The vertical dotted lines indicate the signal region (see text).

4 Statistical analysis and systematic uncertainties

The branching ratio $\mathcal{B}$ of the decay $t \to c(u)H$ is determined in a fit to data by using a likelihood function, L, which is the product of the likelihoods for the four channels (hadronic and leptonic selections, each with two categories). Hypothesised values of $\mathcal{B}$ are probed with a test statistic based on the profile likelihood ratio [73]. For the hadronic selection a fit to the $m_{\gamma\gamma}$ distributions in category 1 and category 2 is performed. The analysis in the leptonic selection is based on event counting, for each category, in two $m_{\gamma\gamma}$ regions: the control region (CR), from 100 to 122 GeV and from 129 to 160 GeV, and the signal region.

The theoretical uncertainties are mainly related to the $t\bar{t}$ production cross section, the Higgs boson branching ratio to $\gamma\gamma$, the resonant background from SM processes and the signal generator uncertainties. The experimental and the generator systematic uncertainties are detailed in section 4.4. All of them are introduced as nuisance parameters in the likelihood.

4.1 Expected event yields

The relevant acceptances and expected resulting numbers of events for the $t \to cH$ signal simulation are reported in table 1 for the hadronic and leptonic analyses, taking 0.2% as branching ratio for $t \to cH$.

A fraction of the SM Higgs boson events produced in association with jets (and one lepton) is accepted by the hadronic (leptonic) analysis if the Higgs boson decays into two photons. These events appear as an additional resonant contribution to the sought-for FCNC diphoton signal. All known SM processes, as listed in section 2.3, were simulated to obtain the acceptances for the hadronic and leptonic selections. Summing all channels gives the expected numbers of events listed in table 1. The $t\bar{t}H$ production mode gives the

JHEP10(2017)129

Selection	Hadronic		Leptonic	
Category	1	2	1	2
	Signal $t \to cH$			
Acceptance with stat. unc. [%]	2.89 ± 0.10	4.15 ± 0.12	0.96 ± 0.03	0.27 ± 0.02
Expected events for $\mathcal{B} = 0.2\%$	$7.85^{+0.64}_{-0.67}$	$11.30^{+0.91}_{-0.96}$	$2.60^{+0.21}_{-0.23}$	$0.71^{+0.07}_{-0.07}$
	SM Higgs boson resonant background			
Expected events	$1.17^{+0.09}_{-0.11}$	$3.27^{+0.25}_{-0.27}$	$0.26^{+0.02}_{-0.03}$	$0.23^{+0.02}_{-0.02}$
$t\bar{t}H$ fraction	90%	68%	92%	77%

Table 1. Expected acceptances (including efficiencies) for simulated $t\bar{t}$ events, with $t \to cH$ and $H \to \gamma\gamma$. The corresponding expected numbers of events are also shown, together with those for SM Higgs boson production, followed by $H \to \gamma\gamma$. The fraction of events from the $t\bar{t}H$ channel, dominant in the SM contribution, is also given. The uncertainties in the acceptances are only statistical. The uncertainties in the expected numbers of events include statistical uncertainties and theoretical uncertainties in the cross sections.

dominant contribution for both selections and both categories. The uncertainties include statistical uncertainties and uncertainties in the cross sections, as given in ref. [32].

Dalitz decays (of the type $H \to \gamma f \bar{f}$, where f is a light fermion) are present in both the signal and SM Higgs boson simulations while the 0.23% branching ratio taken for the $H \to \gamma\gamma$ decay does not include these processes. As their acceptance is essentially zero, a consistent normalisation is restored by removing their contribution to the normalisation factor of each simulated sample. No associated uncertainty is assigned.

4.2 Likelihood for the hadronic selection

The (unbinned) likelihood for each hadronic category includes a Poisson term, the product over all events of the expected $m_{\gamma\gamma}$ distribution function (background + signal parameterised as described below), and a term constraining the external parameters (nuisance parameters) to their expected values, within uncertainties, by the product of the corresponding Gaussian factors.

The signal distribution, assumed identical for SM Higgs boson production and the $t \to cH, H \to \gamma\gamma$ signal is described by a double-sided Crystal Ball function (a Gaussian function with power-law tails on both sides) whose parameters are obtained from a fit to the mass spectrum of the simulated FCNC signal. The Crystal Ball function's mean value is shifted by 90 MeV to account for the difference between the measured Higgs boson mass of 125.09 GeV, and the value of 125 GeV used in the signal simulation. The same signal parameterisation is used for the leptonic analysis (see below).

The parameterisations of the background are obtained from the $m_{\gamma\gamma}$ shapes of the $S_{\gamma\gamma j}$ sample. In order to verify that the parameterisations do not induce a spurious signal when fitting the data, the two distributions are smoothed using non-parametric probability density functions [74], and used to generate background-only pseudo-experiments with on average 115 and 445 events for categories 1 and 2, respectively. The contribution from $t\bar{t}\gamma$,

JHEP10(2017)129

which is small and has large statistical fluctuations, is neglected. The corresponding $m_{\gamma\gamma}$ spectra are fitted with different shape parameterisations. For background-only fits a bias is defined as the difference between the true number of events and the fitted number of events in the SR. For signal+background fits, the bias is defined as the fitted number of signal events. The criterion used to select a background parameterisation is that these biases have to be smaller than 10% of the number of signal events at the expected limit or 20% of the expected uncertainty in this number, mainly resulting from the statistical uncertainty in the number of events in the SR. The background-only and signal+background fits give consistent results. Third- and fourth-order polynomial parameterisations were found to satisfy this criterion and the one with fewer free parameters, the third-order polynomial, was chosen. The associated biases are 0.5 and 1.7 events in category 1 and 2, respectively, and are used as a systematic uncertainty in the final fit.

4.3 Likelihood for the leptonic selection

Given the very low observed number of events in each leptonic category, the likelihood for the leptonic channels is simply taken as a Poisson term, for two intervals of the diphoton invariant mass distribution, the SR and the CR. Instead of using a full probability density function, the distribution of the background is controlled by a free parameter α, defined as the ratio of the numbers of background events expected in the SR and CR. The signal, $\sim$ 90% of which is confined to the SR, is controlled by its magnitude, the other free parameter. The α parameter is one of the nuisance parameters, and its uncertainty is estimated by considering its variations as a function of the assumed background shapes. For a uniform $m_{\gamma\gamma}$ distribution $\alpha = 0.13$ is expected. Using the smooth probability density function from the hadronic analysis yields $\alpha \sim 0.17$. The $S_{\gamma\gamma j}$ background remaining after the leptonic selection (see section 3.3), without any b-tagging requirement and summing categories 1 and 2 to enlarge the available sample, gives $\alpha \sim 0.11$. The nominal value chosen in the fit is $\alpha = 0.14$, with a 30% uncertainty.

4.4 Systematic uncertainties

A summary of the systematic uncertainties affecting the signal yields is given in table 2. The impact of these uncertainties (where relevant) on the parameters of the double-sided Crystal Ball functions is also taken into account. Since many of the uncertainties have a small impact and the analysis is statistically limited, uncertainties affecting jet energy scale, b-tagging, $E_{\mathrm{T}}^{\mathrm{miss}}$, photon identification and lepton-related uncertainties have been grouped so as to have only one equivalent nuisance parameter for each of these quantities.

- The uncertainties in the $t\bar{t}$ production cross section, the $H \to \gamma\gamma$ branching ratio and the integrated luminosity, affect only the normalisation of the signal yield.

- The systematic uncertainties in the energy scale ($\sim 0.5\%$) and resolution ($\sim 12\%$) of photons have a very small impact on the signal acceptance, as shown in table 2. They affect more significantly the parameters of the double-sided Crystal Ball functions used to fit the signal line shape.

JHEP10(2017)129

	Systematic uncertainty [%]			
Selection	Hadronic		Leptonic	
Category	1	2	1	2
$t\bar{t}$ production cross section	$^{+4.8}_{-5.5}$			
Branching ratio of the $H \to \gamma\gamma$ decay	5.0			
Luminosity	3.2			
Photon energy scale	0.3	0.5	1.9	0.6
Photon energy resolution	0.3	0.2	0.3	0.6
Photon identification	1.8	1.7	1.7	1.7
Jet energy scale	$^{+7.9}_{-6.5}$	$^{+6.2}_{-4.8}$	$^{+0.8}_{-2.1}$	$^{+4.3}_{-5.2}$
Jet energy resolution	−2.1	3.0	−2.2	3.5
Jet vertex tagging	0.7	0.4	0.3	0.2
b-tagging	3.3	3.6	3.2	6.5
Lepton identification and scale	–	–	0.6	1.2
$E_{\mathrm{T}}^{\mathrm{miss}}$ scale	–	–	$^{+1.1}_{-0.6}$	$^{+1.8}_{-3.9}$
Pile-up reweighting	1.6	1.2	1.5	1.2
QCD scales	1.7	1.6	1.6	3.2
PDFs	0.7	0.5	0.7	0.5
Top quark mass	1.0	1.0	1.0	3.0
Generator	5.7	−5.8	11.7	6.3
ISR/FSR	$^{+0.4}_{-8.2}$	$^{-8.0}_{+3.8}$	$^{-4.4}_{+0.7}$	$^{-1.1}_{+4.3}$
Hadronisation/underlying event	−5.8	9.6	−4.9	23.2

Table 2. Summary of theoretical, experimental and generator (see text) relative uncertainties in the signal yields, for the hadronic and leptonic selections (in percent, per event). The top three rows affect only the normalisation. The uncertainty related to the photon and lepton isolation selections is included in the identification uncertainty.

- The uncertainties related to the photon trigger and identification amount to about 2%, dominated by the identification efficiency uncertainty.

- The systematic uncertainty associated with the jet energy scale [75] is determined by changing each of the parameters to which it is sensitive by one standard deviation in each direction and one at a time, and taking the quadratic sum of all up (down) variations. The upper (lower) rows in the table correspond respectively to the up (down) variations. The same methodology is used for the jet energy resolution. The sign is negative if the yield decreases when the resolution improves.

- The differences in b-tagging efficiency between data and simulation are included in the event weights of the simulated samples. Replacing the corresponding scale factors by

JHEP10(2017)129

the values obtained when adding (subtracting) their uncertainty induces variations of the expected signal yield of the order of 3%. The uncertainty related to the JVT selection is estimated in the same way.

- The uncertainty associated with the lepton energy scale, identification and reconstruction efficiency, averaged for electrons and muons, is about 1%.
- The uncertainty of about 2% associated with $E_{\mathrm{T}}^{\mathrm{miss}}$ was obtained with the same methodology as that used for the jet energy scale, applied to the *soft term* as introduced in section 3.1.
- The pile-up reweighting uncertainty accounts for the variations allowed when reweighting the distribution of the mean number of interactions per bunch crossing, μ, from simulation to data.

The uncertainties in the signal event generation are evaluated as follows:

- The impact of the factorisation and renormalisation scales (QCD scales) on the signal acceptance is obtained by varying them by a factor of 0.5 or 2 with respect to the nominal values.
- The systematic uncertainty associated with the PDF choice is obtained by using the root mean square of the signal acceptance when considering the 100 Monte Carlo replicas available in the NNPDF3.0 set.
- The systematic uncertainty related to the top quark mass uncertainty is obtained from the variation of acceptance observed when reweighting the simulated signal events by the ratio of a Breit-Wigner function at a mass M (between 171 GeV and 174 GeV) to a Breit-Wigner function at a mass of 172.5 GeV (the mass used at event generation). The uncertainty in the Higgs boson mass, now known at $\pm 0.2\%$ [3], has a negligible impact on the result.
- The uncertainty associated with the hard-process generation is obtained by comparing, at particle level,[6] the acceptances obtained with MG5_aMC@NLO and Powheg for the $t\bar{t}$ generation (both interfaced to Pythia 8). The sign of the uncertainty is positive when Powheg gives a larger yield.
- The uncertainty labelled "ISR/FSR" corresponds to the variation of the signal acceptance observed at particle level when the parameters governing QCD initial- and final-state radiation in Pythia 8 are varied within the allowed range [42]. The upper (lower) row in the table corresponds to the up (down) variation of both ISR and FSR.
- The systematic uncertainty associated with the hadronisation and underlying-event modelling is estimated by comparing the acceptances of events generated with MG5_aMC@NLO interfaced to either Pythia 8 or Herwig 7 [76], at particle level. The sign of the uncertainty is positive when the yield from Herwig 7 is larger.

[6] In a particle level simulation, the same reconstruction algorithms as for the full simulation are used (see sections 2.3 and 3.1), but with final state particles as input instead of tracks and clusters.

JHEP10(2017)129

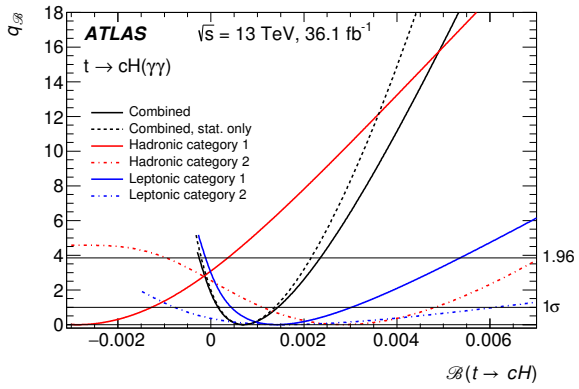

Figure 5. Observed evolution of $q_{\mathcal{B}}$ (see text) as a function of the $t \to cH$ branching ratio $\mathcal{B}$. The dotted curve corresponds to the case where all constrained nuisance parameters are fixed to their maximum-likelihood estimators at $\hat{\mathcal{B}}$. The likelihood functions are only defined for a positive number of expected events, hence the leptonic categories and combined curves do not cover the full scanned range. The intersection of the combined $q_{\mathcal{B}}$ curve with the line at 1.96σ gives the 95% CL upper limit in the asymptotic approximation.

Selection	Hadronic		Leptonic	
Category	1	2	1	2
Signal $t \to cH$	2.4	3.7	0.82	0.23
SM Higgs boson resonant background	1.1	3.1	0.24	0.22
Other background	16	63	0.14	0.29
Total background	17	66	0.38	0.51
Data	14	69	2	1

Table 3. Numbers of FCNC signal events in the SR ($m_{\gamma\gamma} \in [122, 129]$ GeV) for the fitted $t \to cH$ branching ratio $\mathcal{B} = 6.9 \times 10^{-4}$. The numbers of events for the SM Higgs boson production and the fitted non-resonant background are also shown, together with the number of observed events in data, in the four categories.

Finally the uncertainty in the normalisation of the expected yield for the SM Higgs boson production, as a resonant background, is obtained by combining the uncertainties in the individual cross-section predictions (from the renormalisation and factorisation scales, the PDFs and the strong coupling constant, as they are used for table 1), increased to 15% for $t\bar{t}H$, 100% for ggH, VBF and WH, and 50% for the other channels, to account for the fact that the simulations used are not very accurate in the phase space probed by this analysis.

5 Results

Figure 5 shows the evolution of $q_{\mathcal{B}} = -2\left(\ln L(\mathcal{B}) - \ln L(\hat{\mathcal{B}})\right)$ as a function of $\mathcal{B}$ for each category individually, and for the combined likelihood. The fitted branching ratio is $\hat{\mathcal{B}} = 6.9^{+6.8}_{-5.2}(\text{stat.})^{+3.1}_{-1.5}(\text{syst.}) \times 10^{-4}$. A summary of the fitted numbers of signal and background events, together with the numbers of observed events in the SR, is given in table 3.

JHEP10(2017)129

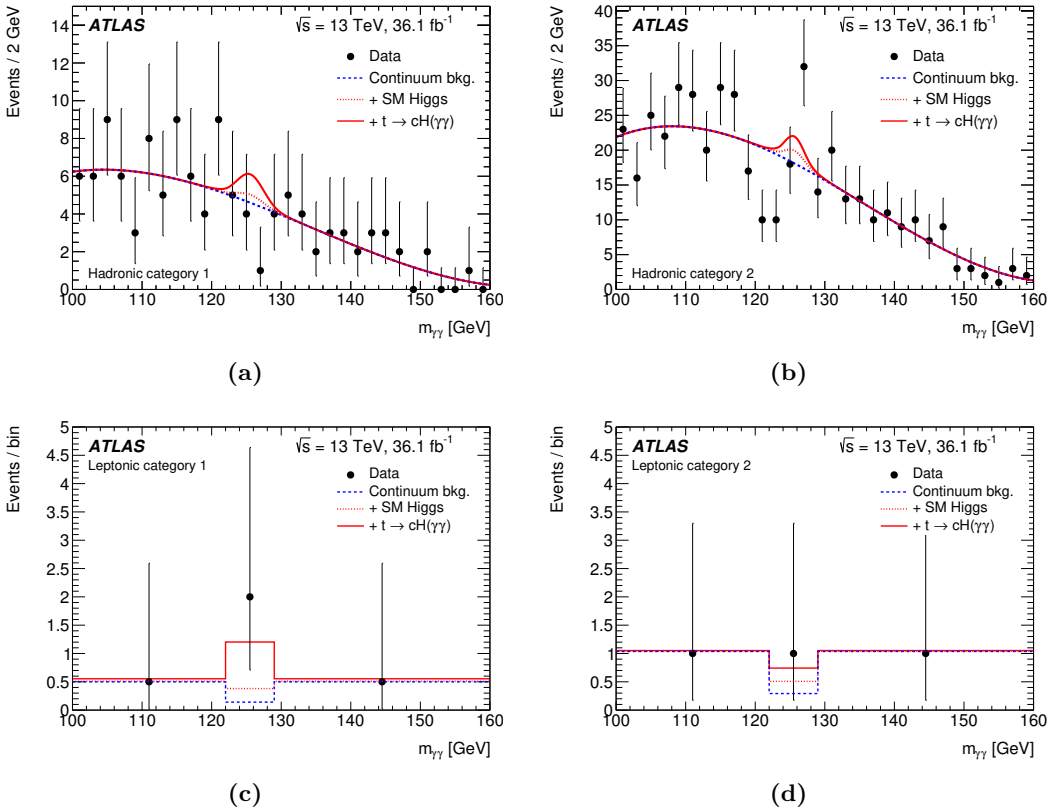

Figure 6. Distributions of $m_{\gamma\gamma}$ for the selected sample in the (a) hadronic category 1, (b) hadronic category 2, (c) leptonic category 1 and (d) leptonic category 2 channels. The result of fitting the data with the sum (full line) of a signal component with the mass of the Higgs boson fixed to $m_H = 125.09\,\text{GeV}$, a continuum background component (dashed line) and the SM Higgs boson contribution (difference between the dotted and dashed lines) is superimposed. The leptonic categories have only two bins: the seven-GeV-wide SR and the CR (see text). The CR region bin extends from the signal region to both higher and lower masses; the content of the CR is shared equally between the low-mass part (100 GeV to 122 GeV) and the high-mass part (129 GeV to 160 GeV) of the CR bin.

The small excesses observed in leptonic category 1 and hadronic category 2 result in minima of their $q_{\mathcal{B}}$ at positive values of $\mathcal{B}$. On the contrary the tight hadronic selection, where a deficit is observed, pulls $\mathcal{B}$ to (unphysical) negative values. The compatibility of the four channels is about 2.3 standard deviations.

The mass distributions corresponding to the result of the combined fit are illustrated for the hadronic and leptonic selections in figure 6. The result of fitting the data with the sum of a signal component and a background component (dashed), described by a third-order polynomial for the hadronic selection, is superimposed. The small contribution from SM Higgs boson production, included in the fit, is also shown (difference between the dotted and dashed lines). For the leptonic channels, the regions $m_{\gamma\gamma} < 122\,\text{GeV}$ and $m_{\gamma\gamma} > 129\,\text{GeV}$ are used as a single-bin control region to estimate the background in the one-bin signal region. For presentation in figure 6, the content of the single-bin CR is shared equally between its low mass part and its high mass part.

JHEP10(2017)129

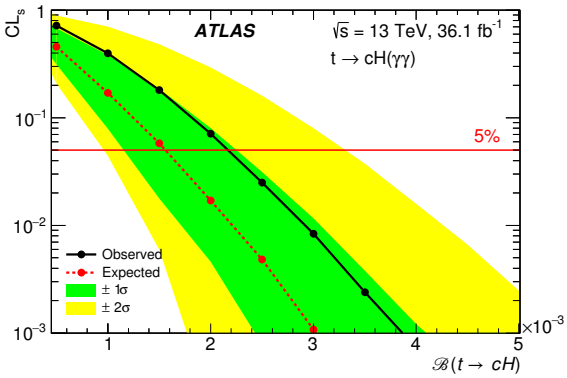

Figure 7. Evolution of the signal confidence level, CL_s, as a function of the $t \to cH$ branching ratio $\mathcal{B}$ for the observation (full line) and the expectation in the absence of signal (dashed line). The bands at $\pm 1\sigma$ and $\pm 2\sigma$ around the expected curve are also shown.

Large-sample pseudo-experiments (which take into account the contribution of the SM Higgs boson production) are used to set the limit on $\mathcal{B}$. The evolution of the signal confidence level CL_s [77] as a function of $\mathcal{B}$, computed from these pseudo-experiments, is shown in figure 7, where the observed result $\mathcal{B} < 2.2 \times 10^{-3}$ at the 95% CL is compared to the expected one in the absence of signal, $\mathcal{B} < 1.6 \times 10^{-3}$. The limit derived from these pseudo-experiments is close to the value obtained, in the asymptotic approximation, from the intersection of the combined $q_{\mathcal{B}}$ curve with the line at 3.84, marking the 95% confidence level. It is dominated by statistical uncertainties, as shown in figure 5.

The acceptance of the $t \to uH$ decays is about 8% lower than for $t \to cH$ in the four analysed channels. The higher acceptance for $t \to cH$ is mostly driven by the additional b-tagging efficiency given by the charm quark as opposed to the up quark. The observed limit for $t \to uH$ is 2.4×10^{-3} and the expected limit is 1.7×10^{-3}, both at the 95% CL.

These limits on $\mathcal{B}$ can be translated to limits on the off-diagonal Yukawa coupling via the relation

$$\lambda_{tqH} = (1.92 \pm 0.02) \times \sqrt{\mathcal{B}},$$

where the mass of the light quark is neglected [33]. The λ_{tqH} coupling corresponds to the sum in quadrature of the couplings relative to the two possible chirality combinations of the quark fields, $\lambda_{tqH} \equiv \sqrt{|\lambda_{t_L q_R}|^2 + |\lambda_{q_L t_R}|^2}$ [78]. The observed (expected) limits are $\lambda_{tcH} < 0.090$ (0.077) and $\lambda_{tuH} < 0.094$ (0.079) at the 95% CL. As the analysis does not distinguish between the two channels, the limit can be written as: $\sqrt{\lambda_{tcH}^2 + 0.92\lambda_{tuH}^2} < 0.090$, where the factor 0.92 is due to the difference in acceptance between the two modes. With this limit ATLAS reaches the sensitivity region where an observation is possible according to models predicting the largest yields (see section 1 and ref. [31]).

6 Conclusions

The FCNC decay of a top quark into a lighter up-type quark ($q = c, u$) and a Higgs boson, $t \to qH$, followed by the decay $H \to \gamma\gamma$, has been searched for in a data set of 36.1 fb^{-1} of 13 TeV proton-proton collisions recorded by the ATLAS experiment at the LHC. The

JHEP10(2017)129

analysis selects events with one top quark decaying into bW (SM decay) and the other into qH. It is split into two final states, targeting the decay of the W boson from the SM top quark decay either in the hadronic mode or in the leptonic mode.

Exploiting the diphoton invariant mass distributions, a sideband technique is used to constrain the background to the sought-for signal. Taking into account the contribution of the SM Higgs boson production, an expected upper limit on the $t \to cH$ decay branching ratio in the absence of signal of 1.6×10^{-3} is estimated. No statistically significant excess is observed in the data, and a limit of 2.2×10^{-3} is set at the 95% CL for $m_H = 125.09\,\text{GeV}$. From this limit, an upper limit on the λ_{tcH} coupling of 0.090 is obtained. As the analysis is almost equally sensitive to the $t \to uH$ mode, the limit obtained can more generally be expressed as $\sqrt{\lambda_{tcH}^2 + 0.92\lambda_{tuH}^2} < 0.090$.

Acknowledgments

We thank CERN for the very successful operation of the LHC, as well as the support staff from our institutions without whom ATLAS could not be operated efficiently.

We acknowledge the support of ANPCyT, Argentina; YerPhI, Armenia; ARC, Australia; BMWFW and FWF, Austria; ANAS, Azerbaijan; SSTC, Belarus; CNPq and FAPESP, Brazil; NSERC, NRC and CFI, Canada; CERN; CONICYT, Chile; CAS, MOST and NSFC, China; COLCIENCIAS, Colombia; MSMT CR, MPO CR and VSC CR, Czech Republic; DNRF and DNSRC, Denmark; IN2P3-CNRS, CEA-DSM/IRFU, France; SRNSF, Georgia; BMBF, HGF, and MPG, Germany; GSRT, Greece; RGC, Hong Kong SAR, China; ISF, I-CORE and Benoziyo Center, Israel; INFN, Italy; MEXT and JSPS, Japan; CNRST, Morocco; NWO, Netherlands; RCN, Norway; MNiSW and NCN, Poland; FCT, Portugal; MNE/IFA, Romania; MES of Russia and NRC KI, Russian Federation; JINR; MESTD, Serbia; MSSR, Slovakia; ARRS and MIZŠ, Slovenia; DST/NRF, South Africa; MINECO, Spain; SRC and Wallenberg Foundation, Sweden; SERI, SNSF and Cantons of Bern and Geneva, Switzerland; MOST, Taiwan; TAEK, Turkey; STFC, United Kingdom; DOE and NSF, United States of America. In addition, individual groups and members have received support from BCKDF, the Canada Council, CANARIE, CRC, Compute Canada, FQRNT, and the Ontario Innovation Trust, Canada; EPLANET, ERC, ERDF, FP7, Horizon 2020 and Marie Skłodowska-Curie Actions, European Union; Investissements d'Avenir Labex and Idex, ANR, Région Auvergne and Fondation Partager le Savoir, France; DFG and AvH Foundation, Germany; Herakleitos, Thales and Aristeia programmes co-financed by EU-ESF and the Greek NSRF; BSF, GIF and Minerva, Israel; BRF, Norway; CERCA Programme Generalitat de Catalunya, Generalitat Valenciana, Spain; the Royal Society and Leverhulme Trust, United Kingdom.

The crucial computing support from all WLCG partners is acknowledged gratefully, in particular from CERN, the ATLAS Tier-1 facilities at TRIUMF (Canada), NDGF (Denmark, Norway, Sweden), CC-IN2P3 (France), KIT/GridKA (Germany), INFN-CNAF (Italy), NL-T1 (Netherlands), PIC (Spain), ASGC (Taiwan), RAL (U.K.) and BNL (U.S.A.), the Tier-2 facilities worldwide and large non-WLCG resource providers. Major contributors of computing resources are listed in ref. [79].

JHEP10(2017)129

References

[1] ATLAS collaboration, *Observation of a new particle in the search for the Standard Model Higgs boson with the ATLAS detector at the LHC*, *Phys. Lett.* **B 716** (2012) 1 [arXiv:1207.7214] [INSPIRE].

[2] CMS collaboration, *Observation of a new boson at a mass of 125 GeV with the CMS experiment at the LHC*, *Phys. Lett.* **B 716** (2012) 30 [arXiv:1207.7235] [INSPIRE].

[3] ATLAS, CMS collaborations, *Combined Measurement of the Higgs Boson Mass in pp Collisions at $\sqrt{s} = 7$ and 8 TeV with the ATLAS and CMS Experiments*, *Phys. Rev. Lett.* **114** (2015) 191803 [arXiv:1503.07589] [INSPIRE].

[4] S.L. Glashow, J. Iliopoulos and L. Maiani, *Weak Interactions with Lepton-Hadron Symmetry*, *Phys. Rev.* **D 2** (1970) 1285 [INSPIRE].

[5] J.A. Aguilar-Saavedra, *Top flavor-changing neutral interactions: Theoretical expectations and experimental detection*, *Acta Phys. Polon.* **B 35** (2004) 2695 [hep-ph/0409342] [INSPIRE].

[6] J.A. Aguilar-Saavedra and B.M. Nobre, *Rare top decays $t \to c\gamma, t \to cg$ and CKM unitarity*, *Phys. Lett.* **B 553** (2003) 251 [hep-ph/0210360] [INSPIRE].

[7] F. del Aguila, J.A. Aguilar-Saavedra and R. Miquel, *Constraints on top couplings in models with exotic quarks*, *Phys. Rev. Lett.* **82** (1999) 1628 [hep-ph/9808400] [INSPIRE].

[8] J.A. Aguilar-Saavedra, *Effects of mixing with quark singlets*, *Phys. Rev.* **D 67** (2003) 035003 [*Erratum ibid.* **D 69** (2004) 099901] [hep-ph/0210112] [INSPIRE].

[9] T.P. Cheng and M. Sher, *Mass Matrix Ansatz and Flavor Nonconservation in Models with Multiple Higgs Doublets*, *Phys. Rev.* **D 35** (1987) 3484 [INSPIRE].

[10] B. Grzadkowski, J.F. Gunion and P. Krawczyk, *Neutral current flavor changing decays for the Z boson and the top quark in two Higgs doublet models*, *Phys. Lett.* **B 268** (1991) 106 [INSPIRE].

[11] M.E. Luke and M.J. Savage, *Flavor changing neutral currents in the Higgs sector and rare top decays*, *Phys. Lett.* **B 307** (1993) 387 [hep-ph/9303249] [INSPIRE].

[12] D. Atwood, L. Reina and A. Soni, *Probing flavor changing top-charm-scalar interactions in e^+e^- collisions*, *Phys. Rev.* **D 53** (1996) 1199 [hep-ph/9506243] [INSPIRE].

[13] D. Atwood, L. Reina and A. Soni, *Phenomenology of two Higgs doublet models with flavor changing neutral currents*, *Phys. Rev.* **D 55** (1997) 3156 [hep-ph/9609279] [INSPIRE].

[14] S. Bejar, J. Guasch and J. Solà, *Loop induced flavor changing neutral decays of the top quark in a general two Higgs doublet model*, *Nucl. Phys.* **B 600** (2001) 21 [hep-ph/0011091] [INSPIRE].

[15] I. Baum, G. Eilam and S. Bar-Shalom, *Scalar flavor changing neutral currents and rare top quark decays in a two H iggs doublet model 'for the top quark'*, *Phys. Rev.* **D 77** (2008) 113008 [arXiv:0802.2622] [INSPIRE].

[16] K.-F. Chen, W.-S. Hou, C. Kao and M. Kohda, *When the Higgs meets the Top: Search for $t \to ch^0$ at the LHC*, *Phys. Lett.* **B 725** (2013) 378 [arXiv:1304.8037] [INSPIRE].

JHEP10(2017)129

[17] D. Atwood, S.K. Gupta and A. Soni, *Constraining the flavor changing Higgs couplings to the top-quark at the LHC*, *JHEP* **10** (2014) 57 [arXiv:1305.2427] [INSPIRE].

[18] C.S. Li, R.J. Oakes and J.M. Yang, *Rare decay of the top quark in the minimal supersymmetric model*, *Phys. Rev.* **D 49** (1994) 293 [*Erratum ibid.* **D 56** (1997) 3156] [INSPIRE].

[19] G.M. de Divitiis, R. Petronzio and L. Silvestrini, *Flavor changing top decays in supersymmetric extensions of the standard model*, *Nucl. Phys.* **B 504** (1997) 45 [hep-ph/9704244] [INSPIRE].

[20] J.L. Lopez, D.V. Nanopoulos and R. Rangarajan, *New supersymmetric contributions to $t \to cV$*, *Phys. Rev.* **D 56** (1997) 3100 [hep-ph/9702350] [INSPIRE].

[21] J. Guasch and J. Solà, *FCNC top quark decays: A door to SUSY physics in high luminosity colliders?*, *Nucl. Phys.* **B 562** (1999) 3 [hep-ph/9906268] [INSPIRE].

[22] D. Delepine and S. Khalil, *Top flavor violating decays in general supersymmetric models*, *Phys. Lett.* **B 599** (2004) 62 [hep-ph/0406264] [INSPIRE].

[23] J.J. Liu, C.S. Li, L.L. Yang and L.G. Jin, *$t \to cV$ via SUSY FCNC couplings in the unconstrained MSSM*, *Phys. Lett.* **B 599** (2004) 92 [hep-ph/0406155] [INSPIRE].

[24] J.J. Cao et al., *SUSY-induced FCNC top-quark processes at the large hadron collider*, *Phys. Rev.* **D 75** (2007) 075021 [hep-ph/0702264] [INSPIRE].

[25] J.M. Yang, B.-L. Young and X. Zhang, *Flavor changing top quark decays in r parity violating SUSY*, *Phys. Rev.* **D 58** (1998) 055001 [hep-ph/9705341] [INSPIRE].

[26] G.-r. Lu, F.-r. Yin, X.-l. Wang and L.-d. Wan, *The Rare top quark decays $t \to cV$ in the topcolor-assisted technicolor model*, *Phys. Rev.* **D 68** (2003) 015002 [hep-ph/0303122] [INSPIRE].

[27] K. Agashe, G. Perez and A. Soni, *Flavor structure of warped extra dimension models*, *Phys. Rev.* **D 71** (2005) 016002 [hep-ph/0408134] [INSPIRE].

[28] K. Agashe, G. Perez and A. Soni, *Collider Signals of Top Quark Flavor Violation from a Warped Extra Dimension*, *Phys. Rev.* **D 75** (2007) 015002 [hep-ph/0606293] [INSPIRE].

[29] K. Agashe and R. Contino, *Composite Higgs-Mediated FCNC*, *Phys. Rev.* **D 80** (2009) 075016 [arXiv:0906.1542] [INSPIRE].

[30] B. Yang, N. Liu and J. Han, *Top quark flavor-changing neutral-current decay to a 125 GeV Higgs boson in the littlest Higgs model with T parity*, *Phys. Rev.* **D 89** (2014) 034020 [arXiv:1308.4852] [INSPIRE].

[31] Top Quark Working Group collaboration, K. Agashe et al., *Working Group Report: Top Quark*, arXiv:1311.2028 [INSPIRE].

[32] LHC Higgs Cross section Working Group collaboration, D. de Florian et al., *Handbook of LHC Higgs Cross sections: 4. Deciphering the Nature of the Higgs Sector*, arXiv:1610.07922 [INSPIRE].

[33] ATLAS collaboration, *Search for top quark decays $t \to qH$ with $H \to \gamma\gamma$ using the ATLAS detector*, *JHEP* **06** (2014) 008 [arXiv:1403.6293] [INSPIRE].

[34] ATLAS collaboration, *Search for flavour-changing neutral current top quark decays $t \to Hq$ in pp collisions at $\sqrt{s} = 8$ TeV with the ATLAS detector*, *JHEP* **12** (2015) 061 [arXiv:1509.06047] [INSPIRE].

JHEP10(2017)129

[35] CMS collaboration, *Search for top quark decays via Higgs-boson-mediated flavor-changing neutral currents in pp collisions at $\sqrt{s} = 8$ TeV*, *JHEP* **02** (2017) 079 [arXiv:1610.04857] [INSPIRE].

[36] ATLAS collaboration, *The ATLAS Experiment at the CERN Large Hadron Collider*, 2008 *JINST* **3** S08003 [INSPIRE].

[37] ATLAS collaboration, *ATLAS Insertable B-Layer Technical Design Report*, ATLAS-TDR-19 (2010).

[38] ATLAS collaboration, *ATLAS Insertable B-Layer Technical Design Report Addendum*, ATLAS-TDR-19-ADD-1 (2012).

[39] ATLAS collaboration, *Luminosity determination in pp collisions at $\sqrt{s} = 8$ TeV using the ATLAS detector at the LHC*, *Eur. Phys. J.* **C 76** (2016) 653 [arXiv:1608.03953] [INSPIRE].

[40] J. Alwall et al., *The automated computation of tree-level and next-to-leading order differential cross sections and their matching to parton shower simulations*, *JHEP* **07** (2014) 079 [arXiv:1405.0301] [INSPIRE].

[41] T. Sjöstrand, S. Mrenna and P.Z. Skands, *A Brief Introduction to PYTHIA 8.1*, *Comput. Phys. Commun.* **178** (2008) 852 [arXiv:0710.3820] [INSPIRE].

[42] ATLAS collaboration, *ATLAS Run 1 PYTHIA8 tunes*, ATL-PHYS-PUB-2014-021 (2014).

[43] C. Degrande, F. Maltoni, J. Wang and C. Zhang, *Automatic computations at next-to-leading order in QCD for top-quark flavor-changing neutral processes*, *Phys. Rev.* **D 91** (2015) 034024 [arXiv:1412.5594] [INSPIRE].

[44] NNPDF collaboration, R.D. Ball et al., *Parton distributions for the LHC Run II*, *JHEP* **04** (2015) 040 [arXiv:1410.8849] [INSPIRE].

[45] M. Czakon, P. Fiedler and A. Mitov, *Total Top-Quark Pair-Production Cross section at Hadron Colliders Through $\mathcal{O}(\alpha_S^4)$*, *Phys. Rev. Lett.* **110** (2013) 252004 [arXiv:1303.6254] [INSPIRE].

[46] M. Czakon and A. Mitov, *Top++: A program for the calculation of the top-pair cross-section at hadron colliders*, *Comput. Phys. Commun.* **185** (2014) 2930 [arXiv:1112.5675] [INSPIRE].

[47] ATLAS collaboration, *Measurement of fiducial, differential and production cross sections in the $H \to \gamma\gamma$ decay channel with 13.3 fb^{-1} of 13 TeV proton-proton collision data with the ATLAS detector*, ATLAS-CONF-2016-067 (2016).

[48] F. Demartin, B. Maier, F. Maltoni, K. Mawatari and M. Zaro, *tWH associated production at the LHC*, *Eur. Phys. J.* **C 77** (2017) 34 [arXiv:1607.05862] [INSPIRE].

[49] S. Alioli, P. Nason, C. Oleari and E. Re, *NLO Higgs boson production via gluon fusion matched with shower in POWHEG*, *JHEP* **04** (2009) 002 [arXiv:0812.0578] [INSPIRE].

[50] P. Nason and C. Oleari, *NLO Higgs boson production via vector-boson fusion matched with shower in POWHEG*, *JHEP* **02** (2010) 037 [arXiv:0911.5299] [INSPIRE].

[51] ATLAS collaboration, *Measurement of the Z/γ^* boson transverse momentum distribution in pp collisions at $\sqrt{s} = 7$ TeV with the ATLAS detector*, *JHEP* **09** (2014) 145 [arXiv:1406.3660] [INSPIRE].

[52] H.-L. Lai et al., *New parton distributions for collider physics*, *Phys. Rev.* **D 82** (2010) 074024 [arXiv:1007.2241] [INSPIRE].

JHEP10(2017)129

[53] P.M. Nadolsky et al., *Implications of CTEQ global analysis for collider observables*, *Phys. Rev.* **D 78** (2008) 013004 [arXiv:0802.0007] [INSPIRE].

[54] T. Gleisberg, S. Hoeche, F. Krauss, M. Schonherr, S. Schumann, F. Siegert et al., *Event generation with SHERPA 1.1*, *JHEP* **02** (2009) 007 [arXiv:0811.4622] [INSPIRE].

[55] ATLAS collaboration, *The ATLAS Simulation Infrastructure*, *Eur. Phys. J.* **C 70** (2010) 823 [arXiv:1005.4568] [INSPIRE].

[56] GEANT4 collaboration, S. Agostinelli et al., *GEANT4: A simulation toolkit*, *Nucl. Instrum. Meth.* **A 506** (2003) 250 [INSPIRE].

[57] ATLAS collaboration, *Measurement of the photon identification efficiencies with the ATLAS detector using LHC Run-1 data*, *Eur. Phys. J.* **C 76** (2016) 666 [arXiv:1606.01813] [INSPIRE].

[58] ATLAS collaboration, *Electron and photon energy calibration with the ATLAS detector using LHC Run 1 data*, *Eur. Phys. J.* **C 74** (2014) 3071 [arXiv:1407.5063] [INSPIRE].

[59] ATLAS collaboration, *Electron and photon energy calibration with the ATLAS detector using data collected in 2015 at* $\sqrt{s} = 13$ *TeV*, ATLAS-PHYS-PUB-2016-015 (2016).

[60] ATLAS collaboration, *Photon identification in 2015 ATLAS data*, ATLAS-PHYS-PUB-2016-014 (2016).

[61] ATLAS collaboration, *Topological cell clustering in the ATLAS calorimeters and its performance in LHC Run 1*, *Eur. Phys. J.* **C 77** (2017) 490 [arXiv:1603.02934] [INSPIRE].

[62] M. Cacciari and G.P. Salam, *Pileup subtraction using jet areas*, *Phys. Lett.* **B 659** (2008) 119 [arXiv:0707.1378] [INSPIRE].

[63] ATLAS collaboration, *Measurement of Higgs boson production in the diphoton decay channel in pp collisions at center-of-mass energies of* 7 *and* 8 *TeV with the ATLAS detector*, *Phys. Rev.* **D 90** (2014) 112015 [arXiv:1408.7084] [INSPIRE].

[64] M. Cacciari, G.P. Salam and G. Soyez, *The anti-*k_t *jet clustering algorithm*, *JHEP* **04** (2008) 063 [arXiv:0802.1189] [INSPIRE].

[65] ATLAS collaboration, *Performance of pile-up mitigation techniques for jets in pp collisions at* $\sqrt{s} = 8$ *TeV using the ATLAS detector*, *Eur. Phys. J.* **C 76** (2016) 581 [arXiv:1510.03823] [INSPIRE].

[66] ATLAS collaboration, *Optimisation of the ATLAS b-tagging performance for the 2016 LHC Run*, ATL-PHYS-PUB-2016-012 (2016).

[67] ATLAS collaboration, *Performance of b-Jet Identification in the ATLAS Experiment*, 2016 *JINST* **11** P04008 [arXiv:1512.01094] [INSPIRE].

[68] ATLAS collaboration, *Electron performance measurements with the ATLAS detector using the 2010 LHC proton-proton collision data*, *Eur. Phys. J.* **C 72** (2012) 1909 [arXiv:1110.3174] [INSPIRE].

[69] ATLAS collaboration, *Electron efficiency measurements with the ATLAS detector using 2012 LHC proton-proton collision data*, *Eur. Phys. J.* **C 77** (2017) 195 [arXiv:1612.01456] [INSPIRE].

[70] ATLAS collaboration, *Electron efficiency measurements with the ATLAS detector using the 2015 LHC proton-proton collision data*, ATLAS-CONF-2016-024 (2016).

JHEP10(2017)129

[71] ATLAS collaboration, *Muon reconstruction performance of the ATLAS detector in proton-proton collision data at* $\sqrt{s} = 13$ *TeV*, *Eur. Phys. J.* **C 76** (2016) 292 [arXiv:1603.05598] [INSPIRE].

[72] ATLAS collaboration, *Performance of algorithms that reconstruct missing transverse momentum in* $\sqrt{s} = 8$ *TeV proton-proton collisions in the ATLAS detector*, *Eur. Phys. J.* **C 77** (2017) 241 [arXiv:1609.09324] [INSPIRE].

[73] G. Cowan, K. Cranmer, E. Gross and O. Vitells, *Asymptotic formulae for likelihood-based tests of new physics*, *Eur. Phys. J.* **C 71** (2011) 1554 [*Erratum ibid.* **C 73** (2013) 2501] [arXiv:1007.1727] [INSPIRE].

[74] K.S. Cranmer, *Kernel estimation in high-energy physics*, *Comput. Phys. Commun.* **136** (2001) 198 [hep-ex/0011057] [INSPIRE].

[75] ATLAS collaboration, *Jet energy scale measurements and their systematic uncertainties in proton-proton collisions at* $\sqrt{s} = 13$ *TeV with the ATLAS detector*, arXiv:1703.09665 [INSPIRE].

[76] J. Bellm et al., *HERWIG 7.0/HERWIG++ 3.0 release note*, *Eur. Phys. J.* **C 76** (2016) 196 [arXiv:1512.01178] [INSPIRE].

[77] A.L. Read, *Presentation of search results: The* CL_s *technique*, *J. Phys.* **G 28** (2002) 2693 [INSPIRE].

[78] R. Harnik, J. Kopp and J. Zupan, *Flavor Violating Higgs Decays*, *JHEP* **03** (2013) 026 [arXiv:1209.1397] [INSPIRE].

[79] ATLAS collaboration, *ATLAS Computing Acknowledgements 2016–2017*, ATL-GEN-PUB-2016-002 (2016).

JHEP10(2017)129

The ATLAS collaboration

M. Aaboud[137d], G. Aad[88], B. Abbott[115], O. Abdinov[12,*], B. Abeloos[119], S.H. Abidi[161], O.S. AbouZeid[139], N.L. Abraham[151], H. Abramowicz[155], H. Abreu[154], R. Abreu[118], Y. Abulaiti[148a,148b], B.S. Acharya[167a,167b,a], S. Adachi[157], L. Adamczyk[41a], J. Adelman[110], M. Adersberger[102], T. Adye[133], A.A. Affolder[139], Y. Afik[154], T. Agatonovic-Jovin[14], C. Agheorghiesei[28c], J.A. Aguilar-Saavedra[128a,128f], S.P. Ahlen[24], F. Ahmadov[68,b], G. Aielli[135a,135b], S. Akatsuka[71], H. Akerstedt[148a,148b], T.P.A. Åkesson[84], E. Akilli[52], A.V. Akimov[98], G.L. Alberghi[22a,22b], J. Albert[172], P. Albicocco[50], M.J. Alconada Verzini[74], S.C. Alderweireldt[108], M. Aleksa[32], I.N. Aleksandrov[68], C. Alexa[28b], G. Alexander[155], T. Alexopoulos[10], M. Alhroob[115], B. Ali[130], M. Aliev[76a,76b], G. Alimonti[94a], J. Alison[33], S.P. Alkire[38], B.M.M. Allbrooke[151], B.W. Allen[118], P.P. Allport[19], A. Aloisio[106a,106b], A. Alonso[39], F. Alonso[74], C. Alpigiani[140], A.A. Alshehri[56], M.I. Alstaty[88], B. Alvarez Gonzalez[32], D. Álvarez Piqueras[170], M.G. Alviggi[106a,106b], B.T. Amadio[16], Y. Amaral Coutinho[26a], C. Amelung[25], D. Amidei[92], S.P. Amor Dos Santos[128a,128c], S. Amoroso[32], G. Amundsen[25], C. Anastopoulos[141], L.S. Ancu[52], N. Andari[19], T. Andeen[11], C.F. Anders[60b], J.K. Anders[77], K.J. Anderson[33], A. Andreazza[94a,94b], V. Andrei[60a], S. Angelidakis[37], I. Angelozzi[109], A. Angerami[38], A.V. Anisenkov[111,c], N. Anjos[13], A. Annovi[126a,126b], C. Antel[60a], M. Antonelli[50], A. Antonov[100,*], D.J. Antrim[166], F. Anulli[134a], M. Aoki[69], L. Aperio Bella[32], G. Arabidze[93], Y. Arai[69], J.P. Araque[128a], V. Araujo Ferraz[26a], A.T.H. Arce[48], R.E. Ardell[80], F.A. Arduh[74], J-F. Arguin[97], S. Argyropoulos[66], M. Arik[20a], A.J. Armbruster[32], L.J. Armitage[79], O. Arnaez[161], H. Arnold[51], M. Arratia[30], O. Arslan[23], A. Artamonov[99,*], G. Artoni[122], S. Artz[86], S. Asai[157], N. Asbah[45], A. Ashkenazi[155], L. Asquith[151], K. Assamagan[27], R. Astalos[146a], M. Atkinson[169], N.B. Atlay[143], K. Augsten[130], G. Avolio[32], B. Axen[16], M.K. Ayoub[119], G. Azuelos[97,d], A.E. Baas[60a], M.J. Baca[19], H. Bachacou[138], K. Bachas[76a,76b], M. Backes[122], P. Bagnaia[134a,134b], M. Bahmani[42], H. Bahrasemani[144], J.T. Baines[133], M. Bajic[39], O.K. Baker[179], E.M. Baldin[111,c], P. Balek[175], F. Balli[138], W.K. Balunas[124], E. Banas[42], A. Bandyopadhyay[23], Sw. Banerjee[176,e], A.A.E. Bannoura[178], L. Barak[155], E.L. Barberio[91], D. Barberis[53a,53b], M. Barbero[88], T. Barillari[103], M-S Barisits[32], J.T. Barkeloo[118], T. Barklow[145], N. Barlow[30], S.L. Barnes[36c], B.M. Barnett[133], R.M. Barnett[16], Z. Barnovska-Blenessy[36a], A. Baroncelli[136a], G. Barone[25], A.J. Barr[122], L. Barranco Navarro[170], F. Barreiro[85], J. Barreiro Guimarães da Costa[35a], R. Bartoldus[145], A.E. Barton[75], P. Bartos[146a], A. Basalaev[125], A. Bassalat[119,f], R.L. Bates[56], S.J. Batista[161], J.R. Batley[30], M. Battaglia[139], M. Bauce[134a,134b], F. Bauer[138], H.S. Bawa[145,g], J.B. Beacham[113], M.D. Beattie[75], T. Beau[83], P.H. Beauchemin[165], P. Bechtle[23], H.P. Beck[18,h], H.C. Beck[57], K. Becker[122], M. Becker[86], C. Becot[112], A.J. Beddall[20e], A. Beddall[20b], V.A. Bednyakov[68], M. Bedognetti[109], C.P. Bee[150], T.A. Beermann[32], M. Begalli[26a], M. Begel[27], J.K. Behr[45], A.S. Bell[81], G. Bella[155], L. Bellagamba[22a], A. Bellerive[31], M. Bellomo[154], K. Belotskiy[100], O. Beltramello[32], N.L. Belyaev[100], O. Benary[155,*], D. Benchekroun[137a], M. Bender[102], K. Bendtz[148a,148b], N. Benekos[10], Y. Benhammou[155], E. Benhar Noccioli[179], J. Benitez[66], D.P. Benjamin[48], M. Benoit[52], J.R. Bensinger[25], S. Bentvelsen[109], L. Beresford[122], M. Beretta[50], D. Berge[109], E. Bergeaas Kuutmann[168], N. Berger[5], J. Beringer[16], S. Berlendis[58], N.R. Bernard[89], G. Bernardi[83], C. Bernius[145], F.U. Bernlochner[23], T. Berry[80], P. Berta[86], C. Bertella[35a], G. Bertoli[148a,148b], F. Bertolucci[126a,126b], I.A. Bertram[75], C. Bertsche[45], D. Bertsche[115], G.J. Besjes[39], O. Bessidskaia Bylund[148a,148b], M. Bessner[45], N. Besson[138], A. Bethani[87], S. Bethke[103], A.J. Bevan[79], J. Beyer[103], R.M. Bianchi[127], O. Biebel[102], D. Biedermann[17], R. Bielski[87], K. Bierwagen[86], N.V. Biesuz[126a,126b], M. Biglietti[136a], T.R.V. Billoud[97], H. Bilokon[50], M. Bindi[57], A. Bingul[20b], C. Bini[134a,134b], S. Biondi[22a,22b], T. Bisanz[57], C. Bittrich[47], D.M. Bjergaard[48], J.E. Black[145], K.M. Black[24], R.E. Blair[6],

JHEP10(2017)129

T. Blazek[146a], I. Bloch[45], C. Blocker[25], A. Blue[56], W. Blum[86,*], U. Blumenschein[79], S. Blunier[34a], G.J. Bobbink[109], V.S. Bobrovnikov[111,c], S.S. Bocchetta[84], A. Bocci[48], C. Bock[102], M. Boehler[51], D. Boerner[178], D. Bogavac[102], A.G. Bogdanchikov[111], C. Bohm[148a], V. Boisvert[80], P. Bokan[168,i], T. Bold[41a], A.S. Boldyrev[101], A.E. Bolz[60b], M. Bomben[83], M. Bona[79], M. Boonekamp[138], A. Borisov[132], G. Borissov[75], J. Bortfeldt[32], D. Bortoletto[122], V. Bortolotto[62a,62b,62c], D. Boscherini[22a], M. Bosman[13], J.D. Bossio Sola[29], J. Boudreau[127], J. Bouffard[2], E.V. Bouhova-Thacker[75], D. Boumediene[37], C. Bourdarios[119], S.K. Boutle[56], A. Boveia[113], J. Boyd[32], I.R. Boyko[68], J. Bracinik[19], A. Brandt[8], G. Brandt[57], O. Brandt[60a], U. Bratzler[158], B. Brau[89], J.E. Brau[118], W.D. Breaden Madden[56], K. Brendlinger[45], A.J. Brennan[91], L. Brenner[109], R. Brenner[168], S. Bressler[175], D.L. Briglin[19], T.M. Bristow[49], D. Britton[56], D. Britzger[45], F.M. Brochu[30], I. Brock[23], R. Brock[93], G. Brooijmans[38], T. Brooks[80], W.K. Brooks[34b], J. Brosamer[16], E. Brost[110], J.H Broughton[19], P.A. Bruckman de Renstrom[42], D. Bruncko[146b], A. Bruni[22a], G. Bruni[22a], L.S. Bruni[109], S. Bruno[135a,135b], BH Brunt[30], M. Bruschi[22a], N. Bruscino[23], P. Bryant[33], L. Bryngemark[45], T. Buanes[15], Q. Buat[144], P. Buchholz[143], A.G. Buckley[56], I.A. Budagov[68], F. Buehrer[51], M.K. Bugge[121], O. Bulekov[100], D. Bullock[8], T.J. Burch[110], S. Burdin[77], C.D. Burgard[51], A.M. Burger[5], B. Burghgrave[110], K. Burka[42], S. Burke[133], I. Burmeister[46], J.T.P. Burr[122], E. Busato[37], D. Büscher[51], V. Büscher[86], P. Bussey[56], J.M. Butler[24], C.M. Buttar[56], J.M. Butterworth[81], P. Butti[32], W. Buttinger[27], A. Buzatu[153], A.R. Buzykaev[111,c], S. Cabrera Urbán[170], D. Caforio[130], V.M. Cairo[40a,40b], O. Cakir[4a], N. Calace[52], P. Calafiura[16], A. Calandri[88], G. Calderini[83], P. Calfayan[64], G. Callea[40a,40b], L.P. Caloba[26a], S. Calvente Lopez[85], D. Calvet[37], S. Calvet[37], T.P. Calvet[88], R. Camacho Toro[33], S. Camarda[32], P. Camarri[135a,135b], D. Cameron[121], R. Caminal Armadans[169], C. Camincher[58], S. Campana[32], M. Campanelli[81], A. Camplani[94a,94b], A. Campoverde[143], V. Canale[106a,106b], M. Cano Bret[36c], J. Cantero[116], T. Cao[155], M.D.M. Capeans Garrido[32], I. Caprini[28b], M. Caprini[28b], M. Capua[40a,40b], R.M. Carbone[38], R. Cardarelli[135a], F. Cardillo[51], I. Carli[131], T. Carli[32], G. Carlino[106a], B.T. Carlson[127], L. Carminati[94a,94b], R.M.D. Carney[148a,148b], S. Caron[108], E. Carquin[34b], S. Carrá[94a,94b], G.D. Carrillo-Montoya[32], D. Casadei[19], M.P. Casado[13,j], M. Casolino[13], D.W. Casper[166], R. Castelijn[109], V. Castillo Gimenez[170], N.F. Castro[128a,k], A. Catinaccio[32], J.R. Catmore[121], A. Cattai[32], J. Caudron[23], V. Cavaliere[169], E. Cavallaro[13], D. Cavalli[94a], M. Cavalli-Sforza[13], V. Cavasinni[126a,126b], E. Celebi[20d], F. Ceradini[136a,136b], L. Cerda Alberich[170], A.S. Cerqueira[26b], A. Cerri[151], L. Cerrito[135a,135b], F. Cerutti[16], A. Cervelli[18], S.A. Cetin[20d], A. Chafaq[137a], D. Chakraborty[110], S.K. Chan[59], W.S. Chan[109], Y.L. Chan[62a], P. Chang[169], J.D. Chapman[30], D.G. Charlton[19], C.C. Chau[31], C.A. Chavez Barajas[151], S. Che[113], S. Cheatham[167a,167c], A. Chegwidden[93], S. Chekanov[6], S.V. Chekulaev[163a], G.A. Chelkov[68,l], M.A. Chelstowska[32], C. Chen[67], H. Chen[27], J. Chen[36a], S. Chen[35b], S. Chen[157], X. Chen[35c,m], Y. Chen[70], H.C. Cheng[92], H.J. Cheng[35a], A. Cheplakov[68], E. Cheremushkina[132], R. Cherkaoui El Moursli[137e], E. Cheu[7], K. Cheung[63], L. Chevalier[138], V. Chiarella[50], G. Chiarelli[126a,126b], G. Chiodini[76a], A.S. Chisholm[32], A. Chitan[28b], Y.H. Chiu[172], M.V. Chizhov[68], K. Choi[64], A.R. Chomont[37], S. Chouridou[156], Y.S. Chow[62a], V. Christodoulou[81], M.C. Chu[62a], J. Chudoba[129], A.J. Chuinard[90], J.J. Chwastowski[42], L. Chytka[117], A.K. Ciftci[4a], D. Cinca[46], V. Cindro[78], I.A. Cioara[23], C. Ciocca[22a,22b], A. Ciocio[16], F. Cirotto[106a,106b], Z.H. Citron[175], M. Citterio[94a], M. Ciubancan[28b], A. Clark[52], B.L. Clark[59], M.R. Clark[38], P.J. Clark[49], R.N. Clarke[16], C. Clement[148a,148b], Y. Coadou[88], M. Cobal[167a,167c], A. Coccaro[52], J. Cochran[67], L. Colasurdo[108], B. Cole[38], A.P. Colijn[109], J. Collot[58], T. Colombo[166], P. Conde Muiño[128a,128b], E. Coniavitis[51], S.H. Connell[147b], I.A. Connelly[87], S. Constantinescu[28b], G. Conti[32], F. Conventi[106a,n], M. Cooke[16], A.M. Cooper-Sarkar[122], F. Cormier[171], K.J.R. Cormier[161], M. Corradi[134a,134b], F. Corriveau[90,o], A. Cortes-Gonzalez[32],

JHEP10(2017)129

G. Cortiana[103], G. Costa[94a], M.J. Costa[170], D. Costanzo[141], G. Cottin[30], G. Cowan[80], B.E. Cox[87], K. Cranmer[112], S.J. Crawley[56], R.A. Creager[124], G. Cree[31], S. Crépé-Renaudin[58], F. Crescioli[83], W.A. Cribbs[148a,148b], M. Cristinziani[23], V. Croft[112], G. Crosetti[40a,40b], A. Cueto[85], T. Cuhadar Donszelmann[141], A.R. Cukierman[145], J. Cummings[179], M. Curatolo[50], J. Cúth[86], S. Czekierda[42], P. Czodrowski[32], G. D'amen[22a,22b], S. D'Auria[56], L. D'eramo[83], M. D'Onofrio[77], M.J. Da Cunha Sargedas De Sousa[128a,128b], C. Da Via[87], W. Dabrowski[41a], T. Dado[146a], T. Dai[92], O. Dale[15], F. Dallaire[97], C. Dallapiccola[89], M. Dam[39], J.R. Dandoy[124], M.F. Daneri[29], N.P. Dang[176], A.C. Daniells[19], N.S. Dann[87], M. Danninger[171], M. Dano Hoffmann[138], V. Dao[150], G. Darbo[53a], S. Darmora[8], J. Dassoulas[3], A. Dattagupta[118], T. Daubney[45], W. Davey[23], C. David[45], T. Davidek[131], D.R. Davis[48], P. Davison[81], E. Dawe[91], I. Dawson[141], K. De[8], R. de Asmundis[106a], A. De Benedetti[115], S. De Castro[22a,22b], S. De Cecco[83], N. De Groot[108], P. de Jong[109], H. De la Torre[93], F. De Lorenzi[67], A. De Maria[57], D. De Pedis[134a], A. De Salvo[134a], U. De Sanctis[135a,135b], A. De Santo[151], K. De Vasconcelos Corga[88], J.B. De Vivie De Regie[119], R. Debbe[27], C. Debenedetti[139], D.V. Dedovich[68], N. Dehghanian[3], I. Deigaard[109], M. Del Gaudio[40a,40b], J. Del Peso[85], D. Delgove[119], F. Deliot[138], C.M. Delitzsch[7], A. Dell'Acqua[32], L. Dell'Asta[24], M. Dell'Orso[126a,126b], M. Della Pietra[106a,106b], D. della Volpe[52], M. Delmastro[5], C. Delporte[119], P.A. Delsart[58], D.A. DeMarco[161], S. Demers[179], M. Demichev[68], A. Demilly[83], S.P. Denisov[132], D. Denysiuk[138], D. Derendarz[42], J.E. Derkaoui[137d], F. Derue[83], P. Dervan[77], K. Desch[23], C. Deterre[45], K. Dette[161], M.R. Devesa[29], P.O. Deviveiros[32], A. Dewhurst[133], S. Dhaliwal[25], F.A. Di Bello[52], A. Di Ciaccio[135a,135b], L. Di Ciaccio[5], W.K. Di Clemente[124], C. Di Donato[106a,106b], A. Di Girolamo[32], B. Di Girolamo[32], B. Di Micco[136a,136b], R. Di Nardo[32], K.F. Di Petrillo[59], A. Di Simone[51], R. Di Sipio[161], D. Di Valentino[31], C. Diaconu[88], M. Diamond[161], F.A. Dias[39], M.A. Diaz[34a], E.B. Diehl[92], J. Dietrich[17], S. Díez Cornell[45], A. Dimitrievska[14], J. Dingfelder[23], P. Dita[28b], S. Dita[28b], F. Dittus[32], F. Djama[88], T. Djobava[54b], J.I. Djuvsland[60a], M.A.B. do Vale[26c], D. Dobos[32], M. Dobre[28b], C. Doglioni[84], J. Dolejsi[131], Z. Dolezal[131], M. Donadelli[26d], S. Donati[126a,126b], P. Dondero[123a,123b], J. Donini[37], J. Dopke[133], A. Doria[106a], M.T. Dova[74], A.T. Doyle[56], E. Drechsler[57], M. Dris[10], Y. Du[36b], J. Duarte-Campderros[155], A. Dubreuil[52], E. Duchovni[175], G. Duckeck[102], A. Ducourthial[83], O.A. Ducu[97,p], D. Duda[109], A. Dudarev[32], A.Chr. Dudder[86], E.M. Duffield[16], L. Duflot[119], M. Dührssen[32], M. Dumancic[175], A.E. Dumitriu[28b], A.K. Duncan[56], M. Dunford[60a], H. Duran Yildiz[4a], M. Düren[55], A. Durglishvili[54b], D. Duschinger[47], B. Dutta[45], D. Duvnjak[1], M. Dyndal[45], B.S. Dziedzic[42], C. Eckardt[45], K.M. Ecker[103], R.C. Edgar[92], T. Eifert[32], G. Eigen[15], K. Einsweiler[16], T. Ekelof[168], M. El Kacimi[137c], R. El Kosseifi[88], V. Ellajosyula[88], M. Ellert[168], S. Elles[5], F. Ellinghaus[178], A.A. Elliot[172], N. Ellis[32], J. Elmsheuser[27], M. Elsing[32], D. Emeliyanov[133], Y. Enari[157], O.C. Endner[86], J.S. Ennis[173], J. Erdmann[46], A. Ereditato[18], M. Ernst[27], S. Errede[169], M. Escalier[119], C. Escobar[170], B. Esposito[50], O. Estrada Pastor[170], A.I. Etienvre[138], E. Etzion[155], H. Evans[64], A. Ezhilov[125], M. Ezzi[137e], F. Fabbri[22a,22b], L. Fabbri[22a,22b], V. Fabiani[108], G. Facini[81], R.M. Fakhrutdinov[132], S. Falciano[134a], R.J. Falla[81], J. Faltova[32], Y. Fang[35a], M. Fanti[94a,94b], A. Farbin[8], A. Farilla[136a], C. Farina[127], E.M. Farina[123a,123b], T. Farooque[93], S. Farrell[16], S.M. Farrington[173], P. Farthouat[32], F. Fassi[137e], P. Fassnacht[32], D. Fassouliotis[9], M. Faucci Giannelli[49], A. Favareto[53a,53b], W.J. Fawcett[122], L. Fayard[119], O.L. Fedin[125,q], W. Fedorko[171], S. Feigl[121], L. Feligioni[88], C. Feng[36b], E.J. Feng[32], H. Feng[92], M.J. Fenton[56], A.B. Fenyuk[132], L. Feremenga[8], P. Fernandez Martinez[170], S. Fernandez Perez[13], J. Ferrando[45], A. Ferrari[168], P. Ferrari[109], R. Ferrari[123a], D.E. Ferreira de Lima[60b], A. Ferrer[170], D. Ferrere[52], C. Ferretti[92], F. Fiedler[86], A. Filipčič[78], M. Filipuzzi[45], F. Filthaut[108], M. Fincke-Keeler[172], K.D. Finelli[152], M.C.N. Fiolhais[128a,128c,r], L. Fiorini[170], A. Fischer[2], C. Fischer[13], J. Fischer[178], W.C. Fisher[93],

JHEP10(2017)129

N. Flaschel[45], I. Fleck[143], P. Fleischmann[92], R.R.M. Fletcher[124], T. Flick[178], B.M. Flierl[102], L.R. Flores Castillo[62a], M.J. Flowerdew[103], G.T. Forcolin[87], A. Formica[138], F.A. Förster[13], A. Forti[87], A.G. Foster[19], D. Fournier[119], H. Fox[75], S. Fracchia[141], P. Francavilla[83], M. Franchini[22a,22b], S. Franchino[60a], D. Francis[32], L. Franconi[121], M. Franklin[59], M. Frate[166], M. Fraternali[123a,123b], D. Freeborn[81], S.M. Fressard-Batraneanu[32], B. Freund[97], D. Froidevaux[32], J.A. Frost[122], C. Fukunaga[158], T. Fusayasu[104], J. Fuster[170], C. Gabaldon[58], O. Gabizon[154], A. Gabrielli[22a,22b], A. Gabrielli[16], G.P. Gach[41a], S. Gadatsch[32], S. Gadomski[80], G. Gagliardi[53a,53b], L.G. Gagnon[97], C. Galea[108], B. Galhardo[128a,128c], E.J. Gallas[122], B.J. Gallop[133], P. Gallus[130], G. Galster[39], K.K. Gan[113], S. Ganguly[37], Y. Gao[77], Y.S. Gao[145,g], F.M. Garay Walls[34a], C. García[170], J.E. García Navarro[170], J.A. García Pascual[35a], M. Garcia-Sciveres[16], R.W. Gardner[33], N. Garelli[145], V. Garonne[121], A. Gascon Bravo[45], K. Gasnikova[45], C. Gatti[50], A. Gaudiello[53a,53b], G. Gaudio[123a], I.L. Gavrilenko[98], C. Gay[171], G. Gaycken[23], E.N. Gazis[10], C.N.P. Gee[133], J. Geisen[57], M. Geisen[86], M.P. Geisler[60a], K. Gellerstedt[148a,148b], C. Gemme[53a], M.H. Genest[58], C. Geng[92], S. Gentile[134a,134b], C. Gentsos[156], S. George[80], D. Gerbaudo[13], A. Gershon[155], G. Geßner[46], S. Ghasemi[143], M. Ghneimat[23], B. Giacobbe[22a], S. Giagu[134a,134b], N. Giangiacomi[22a,22b], P. Giannetti[126a,126b], S.M. Gibson[80], M. Gignac[171], M. Gilchriese[16], D. Gillberg[31], G. Gilles[178], D.M. Gingrich[3,d], M.P. Giordani[167a,167c], F.M. Giorgi[22a], P.F. Giraud[138], P. Giromini[59], G. Giugliarelli[167a,167c], D. Giugni[94a], F. Giuli[122], C. Giuliani[103], M. Giulini[60b], B.K. Gjelsten[121], S. Gkaitatzis[156], I. Gkialas[9,s], E.L. Gkougkousis[13], P. Gkountoumis[10], L.K. Gladilin[101], C. Glasman[85], J. Glatzer[13], P.C.F. Glaysher[45], A. Glazov[45], M. Goblirsch-Kolb[25], J. Godlewski[42], S. Goldfarb[91], T. Golling[52], D. Golubkov[132], A. Gomes[128a,128b,128d], R. Gonçalo[128a], R. Goncalves Gama[26a], J. Goncalves Pinto Firmino Da Costa[138], G. Gonella[51], L. Gonella[19], A. Gongadze[68], S. González de la Hoz[170], S. Gonzalez-Sevilla[52], L. Goossens[32], P.A. Gorbounov[99], H.A. Gordon[27], I. Gorelov[107], B. Gorini[32], E. Gorini[76a,76b], A. Gorišek[78], A.T. Goshaw[48], C. Gössling[46], M.I. Gostkin[68], C.A. Gottardo[23], C.R. Goudet[119], D. Goujdami[137c], A.G. Goussiou[140], N. Govender[147b,t], E. Gozani[154], L. Graber[57], I. Grabowska-Bold[41a], P.O.J. Gradin[168], J. Gramling[166], E. Gramstad[121], S. Grancagnolo[17], V. Gratchev[125], P.M. Gravila[28f], C. Gray[56], H.M. Gray[16], Z.D. Greenwood[82,u], C. Grefe[23], K. Gregersen[81], I.M. Gregor[45], P. Grenier[145], K. Grevtsov[5], J. Griffiths[8], A.A. Grillo[139], K. Grimm[75], S. Grinstein[13,v], Ph. Gris[37], J.-F. Grivaz[119], S. Groh[86], E. Gross[175], J. Grosse-Knetter[57], G.C. Grossi[82], Z.J. Grout[81], A. Grummer[107], L. Guan[92], W. Guan[176], J. Guenther[65], F. Guescini[163a], D. Guest[166], O. Gueta[155], B. Gui[113], E. Guido[53a,53b], T. Guillemin[5], S. Guindon[32], U. Gul[56], C. Gumpert[32], J. Guo[36c], W. Guo[92], Y. Guo[36a], R. Gupta[43], S. Gupta[122], G. Gustavino[115], B.J. Gutelman[154], P. Gutierrez[115], N.G. Gutierrez Ortiz[81], C. Gutschow[81], C. Guyot[138], M.P. Guzik[41a], C. Gwenlan[122], C.B. Gwilliam[77], A. Haas[112], C. Haber[16], H.K. Hadavand[8], N. Haddad[137e], A. Hadef[88], S. Hageböck[23], M. Hagihara[164], H. Hakobyan[180,*], M. Haleem[45], J. Haley[116], G. Halladjian[93], G.D. Hallewell[88], K. Hamacher[178], P. Hamal[117], K. Hamano[172], A. Hamilton[147a], G.N. Hamity[141], P.G. Hamnett[45], L. Han[36a], S. Han[35a], K. Hanagaki[69,w], K. Hanawa[157], M. Hance[139], B. Haney[124], P. Hanke[60a], J.B. Hansen[39], J.D. Hansen[39], M.C. Hansen[23], P.H. Hansen[39], K. Hara[164], A.S. Hard[176], T. Harenberg[178], F. Hariri[119], S. Harkusha[95], P.F. Harrison[173], N.M. Hartmann[102], Y. Hasegawa[142], A. Hasib[49], S. Hassani[138], S. Haug[18], R. Hauser[93], L. Hauswald[47], L.B. Havener[38], M. Havranek[130], C.M. Hawkes[19], R.J. Hawkings[32], D. Hayakawa[159], D. Hayden[93], C.P. Hays[122], J.M. Hays[79], H.S. Hayward[77], S.J. Haywood[133], S.J. Head[19], T. Heck[86], V. Hedberg[84], L. Heelan[8], S. Heer[23], K.K. Heidegger[51], S. Heim[45], T. Heim[16], B. Heinemann[45,x], J.J. Heinrich[102], L. Heinrich[112], C. Heinz[55], J. Hejbal[129], L. Helary[32], A. Held[171], S. Hellman[148a,148b], C. Helsens[32], R.C.W. Henderson[75], Y. Heng[176],

JHEP10(2017)129

S. Henkelmann[171], A.M. Henriques Correia[32], S. Henrot-Versille[119], G.H. Herbert[17], H. Herde[25], V. Herget[177], Y. Hernández Jiménez[147c], H. Herr[86], G. Herten[51], R. Hertenberger[102], L. Hervas[32], T.C. Herwig[124], G.G. Hesketh[81], N.P. Hessey[163a], J.W. Hetherly[43], S. Higashino[69], E. Higón-Rodriguez[170], K. Hildebrand[33], E. Hill[172], J.C. Hill[30], K.H. Hiller[45], S.J. Hillier[19], M. Hils[47], I. Hinchliffe[16], M. Hirose[51], D. Hirschbuehl[178], B. Hiti[78], O. Hladik[129], X. Hoad[49], J. Hobbs[150], N. Hod[163a], M.C. Hodgkinson[141], P. Hodgson[141], A. Hoecker[32], M.R. Hoeferkamp[107], F. Hoenig[102], D. Hohn[23], T.R. Holmes[33], M. Homann[46], S. Honda[164], T. Honda[69], T.M. Hong[127], B.H. Hooberman[169], W.H. Hopkins[118], Y. Horii[105], A.J. Horton[144], J-Y. Hostachy[58], S. Hou[153], A. Hoummada[137a], J. Howarth[87], J. Hoya[74], M. Hrabovsky[117], J. Hrdinka[32], I. Hristova[17], J. Hrivnac[119], T. Hryn'ova[5], A. Hrynevich[96], P.J. Hsu[63], S.-C. Hsu[140], Q. Hu[36a], S. Hu[36c], Y. Huang[35a], Z. Hubacek[130], F. Hubaut[88], F. Huegging[23], T.B. Huffman[122], E.W. Hughes[38], G. Hughes[75], M. Huhtinen[32], P. Huo[150], N. Huseynov[68,b], J. Huston[93], J. Huth[59], G. Iacobucci[52], G. Iakovidis[27], I. Ibragimov[143], L. Iconomidou-Fayard[119], Z. Idrissi[137e], P. Iengo[32], O. Igonkina[109,y], T. Iizawa[174], Y. Ikegami[69], M. Ikeno[69], Y. Ilchenko[11,z], D. Iliadis[156], N. Ilic[145], G. Introzzi[123a,123b], P. Ioannou[9,*], M. Iodice[136a], K. Iordanidou[38], V. Ippolito[59], M.F. Isacson[168], N. Ishijima[120], M. Ishino[157], M. Ishitsuka[159], C. Issever[122], S. Istin[20a], F. Ito[164], J.M. Iturbe Ponce[62a], R. Iuppa[162a,162b], H. Iwasaki[69], J.M. Izen[44], V. Izzo[106a], S. Jabbar[3], P. Jackson[1], R.M. Jacobs[23], V. Jain[2], K.B. Jakobi[86], K. Jakobs[51], S. Jakobsen[65], T. Jakoubek[129], D.O. Jamin[116], D.K. Jana[82], R. Jansky[52], J. Janssen[23], M. Janus[57], P.A. Janus[41a], G. Jarlskog[84], N. Javadov[68,b], T. Javůrek[51], M. Javurkova[51], F. Jeanneau[138], L. Jeanty[16], J. Jejelava[54a,aa], A. Jelinskas[173], P. Jenni[51,ab], C. Jeske[173], S. Jézéquel[5], H. Ji[176], J. Jia[150], H. Jiang[67], Y. Jiang[36a], Z. Jiang[145], S. Jiggins[81], J. Jimenez Pena[170], S. Jin[35a], A. Jinaru[28b], O. Jinnouchi[159], H. Jivan[147c], P. Johansson[141], K.A. Johns[7], C.A. Johnson[64], W.J. Johnson[140], K. Jon-And[148a,148b], R.W.L. Jones[75], S.D. Jones[151], S. Jones[7], T.J. Jones[77], J. Jongmanns[60a], P.M. Jorge[128a,128b], J. Jovicevic[163a], X. Ju[176], A. Juste Rozas[13,v], M.K. Köhler[175], A. Kaczmarska[42], M. Kado[119], H. Kagan[113], M. Kagan[145], S.J. Kahn[88], T. Kaji[174], E. Kajomovitz[48], C.W. Kalderon[84], A. Kaluza[86], S. Kama[43], A. Kamenshchikov[132], N. Kanaya[157], L. Kanjir[78], V.A. Kantserov[100], J. Kanzaki[69], B. Kaplan[112], L.S. Kaplan[176], D. Kar[147c], K. Karakostas[10], N. Karastathis[10], M.J. Kareem[57], E. Karentzos[10], S.N. Karpov[68], Z.M. Karpova[68], K. Karthik[112], V. Kartvelishvili[75], A.N. Karyukhin[132], K. Kasahara[164], L. Kashif[176], R.D. Kass[113], A. Kastanas[149], Y. Kataoka[157], C. Kato[157], A. Katre[52], J. Katzy[45], K. Kawade[70], K. Kawagoe[73], T. Kawamoto[157], G. Kawamura[57], E.F. Kay[77], V.F. Kazanin[111,c], R. Keeler[172], R. Kehoe[43], J.S. Keller[31], E. Kellermann[84], J.J. Kempster[80], J Kendrick[19], H. Keoshkerian[161], O. Kepka[129], B.P. Kerševan[78], S. Kersten[178], R.A. Keyes[90], M. Khader[169], F. Khalil-zada[12], A. Khanov[116], A.G. Kharlamov[111,c], T. Kharlamova[111,c], A. Khodinov[160], T.J. Khoo[52], V. Khovanskiy[99,*], E. Khramov[68], J. Khubua[54b,ac], S. Kido[70], C.R. Kilby[80], H.Y. Kim[8], S.H. Kim[164], Y.K. Kim[33], N. Kimura[156], O.M. Kind[17], B.T. King[77], D. Kirchmeier[47], J. Kirk[133], A.E. Kiryunin[103], T. Kishimoto[157], D. Kisielewska[41a], V. Kitali[45], O. Kivernyk[5], E. Kladiva[146b], T. Klapdor-Kleingrothaus[51], M.H. Klein[38], M. Klein[77], U. Klein[77], K. Kleinknecht[86], P. Klimek[110], A. Klimentov[27], R. Klingenberg[46], T. Klingl[23], T. Klioutchnikova[32], E.-E. Kluge[60a], P. Kluit[109], S. Kluth[103], E. Kneringer[65], E.B.F.G. Knoops[88], A. Knue[103], A. Kobayashi[157], D. Kobayashi[159], T. Kobayashi[157], M. Kobel[47], M. Kocian[145], P. Kodys[131], T. Koffas[31], E. Koffeman[109], N.M. Köhler[103], T. Koi[145], M. Kolb[60b], I. Koletsou[5], A.A. Komar[98,*], T. Kondo[69], N. Kondrashova[36c], K. Köneke[51], A.C. König[108], T. Kono[69,ad], R. Konoplich[112,ae], N. Konstantinidis[81], R. Kopeliansky[64], S. Koperny[41a], A.K. Kopp[51], K. Korcyl[42], K. Kordas[156], A. Korn[81], A.A. Korol[111,c], I. Korolkov[13], E.V. Korolkova[141], O. Kortner[103], S. Kortner[103], T. Kosek[131], V.V. Kostyukhin[23], A. Kotwal[48], A. Koulouris[10],

JHEP10(2017)129

A. Kourkoumeli-Charalampidi[123a,123b], C. Kourkoumelis[9], E. Kourlitis[141], V. Kouskoura[27], A.B. Kowalewska[42], R. Kowalewski[172], T.Z. Kowalski[41a], C. Kozakai[157], W. Kozanecki[138], A.S. Kozhin[132], V.A. Kramarenko[101], G. Kramberger[78], D. Krasnopevtsev[100], M.W. Krasny[83], A. Krasznahorkay[32], D. Krauss[103], J.A. Kremer[41a], J. Kretzschmar[77], K. Kreutzfeldt[55], P. Krieger[161], K. Krizka[16], K. Kroeninger[46], H. Kroha[103], J. Kroll[129], J. Kroll[124], J. Kroseberg[23], J. Krstic[14], U. Kruchonak[68], H. Krüger[23], N. Krumnack[67], M.C. Kruse[48], T. Kubota[91], H. Kucuk[81], S. Kuday[4b], J.T. Kuechler[178], S. Kuehn[32], A. Kugel[60a], F. Kuger[177], T. Kuhl[45], V. Kukhtin[68], R. Kukla[88], Y. Kulchitsky[95], S. Kuleshov[34b], Y.P. Kulinich[169], M. Kuna[134a,134b], T. Kunigo[71], A. Kupco[129], T. Kupfer[46], O. Kuprash[155], H. Kurashige[70], L.L. Kurchaninov[163a], Y.A. Kurochkin[95], M.G. Kurth[35a], V. Kus[129], E.S. Kuwertz[172], M. Kuze[159], J. Kvita[117], T. Kwan[172], D. Kyriazopoulos[141], A. La Rosa[103], J.L. La Rosa Navarro[26d], L. La Rotonda[40a,40b], F. La Ruffa[40a,40b], C. Lacasta[170], F. Lacava[134a,134b], J. Lacey[45], D.P.J. Lack[87], H. Lacker[17], D. Lacour[83], E. Ladygin[68], R. Lafaye[5], B. Laforge[83], T. Lagouri[179], S. Lai[57], S. Lammers[64], W. Lampl[7], E. Lançon[27], U. Landgraf[51], M.P.J. Landon[79], M.C. Lanfermann[52], V.S. Lang[45], J.C. Lange[13], R.J. Langenberg[32], A.J. Lankford[166], F. Lanni[27], K. Lantzsch[23], A. Lanza[123a], A. Lapertosa[53a,53b], S. Laplace[83], J.F. Laporte[138], T. Lari[94a], F. Lasagni Manghi[22a,22b], M. Lassnig[32], T.S. Lau[62a], P. Laurelli[50], W. Lavrijsen[16], A.T. Law[139], P. Laycock[77], T. Lazovich[59], M. Lazzaroni[94a,94b], B. Le[91], O. Le Dortz[83], E. Le Guirriec[88], E.P. Le Quilleuc[138], M. LeBlanc[172], T. LeCompte[6], F. Ledroit-Guillon[58], C.A. Lee[27], G.R. Lee[133,af], S.C. Lee[153], L. Lee[59], B. Lefebvre[90], G. Lefebvre[83], M. Lefebvre[172], F. Legger[102], C. Leggett[16], G. Lehmann Miotto[32], X. Lei[7], W.A. Leight[45], M.A.L. Leite[26d], R. Leitner[131], D. Lellouch[175], B. Lemmer[57], K.J.C. Leney[81], T. Lenz[23], B. Lenzi[32], R. Leone[7], S. Leone[126a,126b], C. Leonidopoulos[49], G. Lerner[151], C. Leroy[97], A.A.J. Lesage[138], C.G. Lester[30], M. Levchenko[125], J. Levêque[5], D. Levin[92], L.J. Levinson[175], M. Levy[19], D. Lewis[79], B. Li[36a,ag], Changqiao Li[36a], H. Li[150], L. Li[36c], Q. Li[35a], Q. Li[36a], S. Li[48], X. Li[36c], Y. Li[143], Z. Liang[35a], B. Liberti[135a], A. Liblong[161], K. Lie[62c], J. Liebal[23], W. Liebig[15], A. Limosani[152], S.C. Lin[182], T.H. Lin[86], R.A. Linck[64], B.E. Lindquist[150], A.E. Lionti[52], E. Lipeles[124], A. Lipniacka[15], M. Lisovyi[60b], T.M. Liss[169,ah], A. Lister[171], A.M. Litke[139], B. Liu[67], H. Liu[92], H. Liu[27], J.K.K. Liu[122], J. Liu[36b], J.B. Liu[36a], K. Liu[88], L. Liu[169], M. Liu[36a], Y.L. Liu[36a], Y. Liu[36a], M. Livan[123a,123b], A. Lleres[58], J. Llorente Merino[35a], S.L. Lloyd[79], C.Y. Lo[62b], F. Lo Sterzo[153], E.M. Lobodzinska[45], P. Loch[7], F.K. Loebinger[87], A. Loesle[51], K.M. Loew[25], A. Loginov[179,*], T. Lohse[17], K. Lohwasser[141], M. Lokajicek[129], B.A. Long[24], J.D. Long[169], R.E. Long[75], L. Longo[76a,76b], K.A. Looper[113], J.A. Lopez[34b], D. Lopez Mateos[59], I. Lopez Paz[13], A. Lopez Solis[83], J. Lorenz[102], N. Lorenzo Martinez[5], M. Losada[21], P.J. Lösel[102], X. Lou[35a], A. Lounis[119], J. Love[6], P.A. Love[75], H. Lu[62a], N. Lu[92], Y.J. Lu[63], H.J. Lubatti[140], C. Luci[134a,134b], A. Lucotte[58], C. Luedtke[51], F. Luehring[64], W. Lukas[65], L. Luminari[134a], O. Lundberg[148a,148b], B. Lund-Jensen[149], M.S. Lutz[89], P.M. Luzi[83], D. Lynn[27], R. Lysak[129], E. Lytken[84], F. Lyu[35a], V. Lyubushkin[68], H. Ma[27], L.L. Ma[36b], Y. Ma[36b], G. Maccarrone[50], A. Macchiolo[103], C.M. Macdonald[141], B. Maček[78], J. Machado Miguens[124,128b], D. Madaffari[170], R. Madar[37], W.F. Mader[47], A. Madsen[45], J. Maeda[70], S. Maeland[15], T. Maeno[27], A.S. Maevskiy[101], V. Magerl[51], J. Mahlstedt[109], C. Maiani[119], C. Maidantchik[26a], A.A. Maier[103], T. Maier[102], A. Maio[128a,128b,128d], O. Majersky[146a], S. Majewski[118], Y. Makida[69], N. Makovec[119], B. Malaescu[83], Pa. Malecki[42], V.P. Maleev[125], F. Malek[58], U. Mallik[66], D. Malon[6], C. Malone[30], S. Maltezos[10], S. Malyukov[32], J. Mamuzic[170], G. Mancini[50], I. Mandić[78], J. Maneira[128a,128b], L. Manhaes de Andrade Filho[26b], J. Manjarres Ramos[47], K.H. Mankinen[84], A. Mann[102], A. Manousos[32], B. Mansoulie[138], J.D. Mansour[35a], R. Mantifel[90], M. Mantoani[57], S. Manzoni[94a,94b], L. Mapelli[32], G. Marceca[29], L. March[52], L. Marchese[122], G. Marchiori[83], M. Marcisovsky[129], C.A. Marin Tobon[32], M. Marjanovic[37], D.E. Marley[92],

JHEP10(2017)129

F. Marroquim[26a], S.P. Marsden[87], Z. Marshall[16], M.U.F Martensson[168], S. Marti-Garcia[170], C.B. Martin[113], T.A. Martin[173], V.J. Martin[49], B. Martin dit Latour[15], M. Martinez[13,v], V.I. Martinez Outschoorn[169], S. Martin-Haugh[133], V.S. Martoiu[28b], A.C. Martyniuk[81], A. Marzin[32], L. Masetti[86], T. Mashimo[157], R. Mashinistov[98], J. Masik[87], A.L. Maslennikov[111,c], L. Massa[135a,135b], P. Mastrandrea[5], A. Mastroberardino[40a,40b], T. Masubuchi[157], P. Mättig[178], J. Maurer[28b], S.J. Maxfield[77], D.A. Maximov[111,c], R. Mazini[153], I. Maznas[156], S.M. Mazza[94a,94b], N.C. Mc Fadden[107], G. Mc Goldrick[161], S.P. Mc Kee[92], A. McCarn[92], R.L. McCarthy[150], T.G. McCarthy[103], L.I. McClymont[81], E.F. McDonald[91], J.A. Mcfayden[32], G. Mchedlidze[57], S.J. McMahon[133], P.C. McNamara[91], C.J. McNicol[173], R.A. McPherson[172,o], S. Meehan[140], T.J. Megy[51], S. Mehlhase[102], A. Mehta[77], T. Meideck[58], K. Meier[60a], B. Meirose[44], D. Melini[170,ai], B.R. Mellado Garcia[147c], J.D. Mellenthin[57], M. Melo[146a], F. Meloni[18], A. Melzer[23], S.B. Menary[87], L. Meng[77], X.T. Meng[92], A. Mengarelli[22a,22b], S. Menke[103], E. Meoni[40a,40b], S. Mergelmeyer[17], C. Merlassino[18], P. Mermod[52], L. Merola[106a,106b], C. Meroni[94a], F.S. Merritt[33], A. Messina[134a,134b], J. Metcalfe[6], A.S. Mete[166], C. Meyer[124], J-P. Meyer[138], J. Meyer[109], H. Meyer Zu Theenhausen[60a], F. Miano[151], R.P. Middleton[133], S. Miglioranzi[53a,53b], L. Mijović[49], G. Mikenberg[175], M. Mikestikova[129], M. Mikuž[78], M. Milesi[91], A. Milic[161], D.A. Millar[79], D.W. Miller[33], C. Mills[49], A. Milov[175], D.A. Milstead[148a,148b], A.A. Minaenko[132], Y. Minami[157], I.A. Minashvili[68], A.I. Mincer[112], B. Mindur[41a], M. Mineev[68], Y. Minegishi[157], Y. Ming[176], L.M. Mir[13], K.P. Mistry[124], T. Mitani[174], J. Mitrevski[102], V.A. Mitsou[170], A. Miucci[18], P.S. Miyagawa[141], A. Mizukami[69], J.U. Mjörnmark[84], T. Mkrtchyan[180], M. Mlynarikova[131], T. Moa[148a,148b], K. Mochizuki[97], P. Mogg[51], S. Mohapatra[38], S. Molander[148a,148b], R. Moles-Valls[23], M.C. Mondragon[93], K. Mönig[45], J. Monk[39], E. Monnier[88], A. Montalbano[150], J. Montejo Berlingen[32], F. Monticelli[74], S. Monzani[94a,94b], R.W. Moore[3], N. Morange[119], D. Moreno[21], M. Moreno Llácer[32], P. Morettini[53a], S. Morgenstern[32], D. Mori[144], T. Mori[157], M. Morii[59], M. Morinaga[174], V. Morisbak[121], A.K. Morley[32], G. Mornacchi[32], J.D. Morris[79], L. Morvaj[150], P. Moschovakos[10], M. Mosidze[54b], H.J. Moss[141], J. Moss[145,aj], K. Motohashi[159], R. Mount[145], E. Mountricha[27], E.J.W. Moyse[89], S. Muanza[88], F. Mueller[103], J. Mueller[127], R.S.P. Mueller[102], D. Muenstermann[75], P. Mullen[56], G.A. Mullier[18], F.J. Munoz Sanchez[87], W.J. Murray[173,133], H. Musheghyan[32], M. Muškinja[78], A.G. Myagkov[132,ak], M. Myska[130], B.P. Nachman[16], O. Nackenhorst[52], K. Nagai[122], R. Nagai[69,ad], K. Nagano[69], Y. Nagasaka[61], K. Nagata[164], M. Nagel[51], E. Nagy[88], A.M. Nairz[32], Y. Nakahama[105], K. Nakamura[69], T. Nakamura[157], I. Nakano[114], R.F. Naranjo Garcia[45], R. Narayan[11], D.I. Narrias Villar[60a], I. Naryshkin[125], T. Naumann[45], G. Navarro[21], R. Nayyar[7], H.A. Neal[92], P.Yu. Nechaeva[98], T.J. Neep[138], A. Negri[123a,123b], M. Negrini[22a], S. Nektarijevic[108], C. Nellist[119], A. Nelson[166], M.E. Nelson[122], S. Nemecek[129], P. Nemethy[112], M. Nessi[32,al], M.S. Neubauer[169], M. Neumann[178], P.R. Newman[19], T.Y. Ng[62c], T. Nguyen Manh[97], R.B. Nickerson[122], R. Nicolaidou[138], J. Nielsen[139], V. Nikolaenko[132,ak], I. Nikolic-Audit[83], K. Nikolopoulos[19], J.K. Nilsen[121], P. Nilsson[27], Y. Ninomiya[157], A. Nisati[134a], N. Nishu[36c], R. Nisius[103], I. Nitsche[46], T. Nitta[174], T. Nobe[157], Y. Noguchi[71], M. Nomachi[120], I. Nomidis[31], M.A. Nomura[27], T. Nooney[79], M. Nordberg[32], N. Norjoharuddeen[122], O. Novgorodova[47], S. Nowak[103], M. Nozaki[69], L. Nozka[117], K. Ntekas[166], E. Nurse[81], F. Nuti[91], K. O'connor[25], D.C. O'Neil[144], A.A. O'Rourke[45], V. O'Shea[56], F.G. Oakham[31,d], H. Oberlack[103], T. Obermann[23], J. Ocariz[83], A. Ochi[70], I. Ochoa[38], J.P. Ochoa-Ricoux[34a], S. Oda[73], S. Odaka[69], A. Oh[87], S.H. Oh[48], C.C. Ohm[16], H. Ohman[168], H. Oide[53a,53b], H. Okawa[164], Y. Okumura[157], T. Okuyama[69], A. Olariu[28b], L.F. Oleiro Seabra[128a], S.A. Olivares Pino[34a], D. Oliveira Damazio[27], A. Olszewski[42], J. Olszowska[42], A. Onofre[128a,128e], K. Onogi[105], P.U.E. Onyisi[11,z], H. Oppen[121], M.J. Oreglia[33], Y. Oren[155], D. Orestano[136a,136b], N. Orlando[62b], R.S. Orr[161],

JHEP10(2017)129

B. Osculati[53a,53b,*], R. Ospanov[36a], G. Otero y Garzon[29], H. Otono[73], M. Ouchrif[137d], F. Ould-Saada[121], A. Ouraou[138], K.P. Oussoren[109], Q. Ouyang[35a], M. Owen[56], R.E. Owen[19], V.E. Ozcan[20a], N. Ozturk[8], K. Pachal[144], A. Pacheco Pages[13], L. Pacheco Rodriguez[138], C. Padilla Aranda[13], S. Pagan Griso[16], M. Paganini[179], F. Paige[27], G. Palacino[64], S. Palazzo[40a,40b], S. Palestini[32], M. Palka[41b], D. Pallin[37], E.St. Panagiotopoulou[10], I. Panagoulias[10], C.E. Pandini[126a,126b], J.G. Panduro Vazquez[80], P. Pani[32], S. Panitkin[27], D. Pantea[28b], L. Paolozzi[52], Th.D. Papadopoulou[10], K. Papageorgiou[9,s], A. Paramonov[6], D. Paredes Hernandez[179], A.J. Parker[75], M.A. Parker[30], K.A. Parker[45], F. Parodi[53a,53b], J.A. Parsons[38], U. Parzefall[51], V.R. Pascuzzi[161], J.M. Pasner[139], E. Pasqualucci[134a], S. Passaggio[53a], Fr. Pastore[80], S. Pataraia[86], J.R. Pater[87], T. Pauly[32], B. Pearson[103], S. Pedraza Lopez[170], R. Pedro[128a,128b], S.V. Peleganchuk[111,c], O. Penc[129], C. Peng[35a], H. Peng[36a], J. Penwell[64], B.S. Peralva[26b], M.M. Perego[138], D.V. Perepelitsa[27], F. Peri[17], L. Perini[94a,94b], H. Pernegger[32], S. Perrella[106a,106b], R. Peschke[45], V.D. Peshekhonov[68,*], K. Peters[45], R.F.Y. Peters[87], B.A. Petersen[32], T.C. Petersen[39], E. Petit[58], A. Petridis[1], C. Petridou[156], P. Petroff[119], E. Petrolo[134a], M. Petrov[122], F. Petrucci[136a,136b], N.E. Pettersson[89], A. Peyaud[138], R. Pezoa[34b], F.H. Phillips[93], P.W. Phillips[133], G. Piacquadio[150], E. Pianori[173], A. Picazio[89], E. Piccaro[79], M.A. Pickering[122], R. Piegaia[29], J.E. Pilcher[33], A.D. Pilkington[87], A.W.J. Pin[87], M. Pinamonti[135a,135b], J.L. Pinfold[3], H. Pirumov[45], M. Pitt[175], L. Plazak[146a], M.-A. Pleier[27], V. Pleskot[86], E. Plotnikova[68], D. Pluth[67], P. Podberezko[111], R. Poettgen[84], R. Poggi[123a,123b], L. Poggioli[119], I. Pogrebnyak[93], D. Pohl[23], G. Polesello[123a], A. Poley[45], A. Policicchio[40a,40b], R. Polifka[32], A. Polini[22a], C.S. Pollard[56], V. Polychronakos[27], K. Pommès[32], D. Ponomarenko[100], L. Pontecorvo[134a], G.A. Popeneciu[28d], S. Pospisil[130], K. Potamianos[16], I.N. Potrap[68], C.J. Potter[30], T. Poulsen[84], J. Poveda[32], M.E. Pozo Astigarraga[32], P. Pralavorio[88], A. Pranko[16], S. Prell[67], D. Price[87], M. Primavera[76a], S. Prince[90], N. Proklova[100], K. Prokofiev[62c], F. Prokoshin[34b], S. Protopopescu[27], J. Proudfoot[6], M. Przybycien[41a], A. Puri[169], P. Puzo[119], J. Qian[92], G. Qin[56], Y. Qin[87], A. Quadt[57], M. Queitsch-Maitland[45], D. Quilty[56], S. Raddum[121], V. Radeka[27], V. Radescu[122], S.K. Radhakrishnan[150], P. Radloff[118], P. Rados[91], F. Ragusa[94a,94b], G. Rahal[181], J.A. Raine[87], S. Rajagopalan[27], C. Rangel-Smith[168], T. Rashid[119], S. Raspopov[5], M.G. Ratti[94a,94b], D.M. Rauch[45], F. Rauscher[102], S. Rave[86], I. Ravinovich[175], J.H. Rawling[87], M. Raymond[32], A.L. Read[121], N.P. Readioff[58], M. Reale[76a,76b], D.M. Rebuzzi[123a,123b], A. Redelbach[177], G. Redlinger[27], R. Reece[139], R.G. Reed[147c], K. Reeves[44], L. Rehnisch[17], J. Reichert[124], A. Reiss[86], C. Rembser[32], H. Ren[35a], M. Rescigno[134a], S. Resconi[94a], E.D. Resseguie[124], S. Rettie[171], E. Reynolds[19], O.L. Rezanova[111,c], P. Reznicek[131], R. Rezvani[97], R. Richter[103], S. Richter[81], E. Richter-Was[41b], O. Ricken[23], M. Ridel[83], P. Rieck[103], C.J. Riegel[178], J. Rieger[57], O. Rifki[115], M. Rijssenbeek[150], A. Rimoldi[123a,123b], M. Rimoldi[18], L. Rinaldi[22a], G. Ripellino[149], B. Ristić[32], E. Ritsch[32], I. Riu[13], F. Rizatdinova[116], E. Rizvi[79], C. Rizzi[13], R.T. Roberts[87], S.H. Robertson[90,o], A. Robichaud-Veronneau[90], D. Robinson[30], J.E.M. Robinson[45], A. Robson[56], E. Rocco[86], C. Roda[126a,126b], Y. Rodina[88,am], S. Rodriguez Bosca[170], A. Rodriguez Perez[13], D. Rodriguez Rodriguez[170], S. Roe[32], C.S. Rogan[59], O. Røhne[121], J. Roloff[59], A. Romaniouk[100], M. Romano[22a,22b], S.M. Romano Saez[37], E. Romero Adam[170], N. Rompotis[77], M. Ronzani[51], L. Roos[83], S. Rosati[134a], K. Rosbach[51], P. Rose[139], N.-A. Rosien[57], E. Rossi[106a,106b], L.P. Rossi[53a], J.H.N. Rosten[30], R. Rosten[140], M. Rotaru[28b], J. Rothberg[140], D. Rousseau[119], A. Rozanov[88], Y. Rozen[154], X. Ruan[147c], F. Rubbo[145], F. Rühr[51], A. Ruiz-Martinez[31], Z. Rurikova[51], N.A. Rusakovich[68], H.L. Russell[90], J.P. Rutherfoord[7], N. Ruthmann[32], Y.F. Ryabov[125], M. Rybar[169], G. Rybkin[119], S. Ryu[6], A. Ryzhov[132], G.F. Rzehorz[57], A.F. Saavedra[152], G. Sabato[109], S. Sacerdoti[29], H.F-W. Sadrozinski[139], R. Sadykov[68], F. Safai Tehrani[134a],

JHEP10(2017)129

P. Saha[110], M. Sahinsoy[60a], M. Saimpert[45], M. Saito[157], T. Saito[157], H. Sakamoto[157], Y. Sakurai[174], G. Salamanna[136a,136b], J.E. Salazar Loyola[34b], D. Salek[109], P.H. Sales De Bruin[168], D. Salihagic[103], A. Salnikov[145], J. Salt[170], D. Salvatore[40a,40b], F. Salvatore[151], A. Salvucci[62a,62b,62c], A. Salzburger[32], D. Sammel[51], D. Sampsonidis[156], D. Sampsonidou[156], J. Sánchez[170], V. Sanchez Martinez[170], A. Sanchez Pineda[167a,167c], H. Sandaker[121], R.L. Sandbach[79], C.O. Sander[45], M. Sandhoff[178], C. Sandoval[21], D.P.C. Sankey[133], M. Sannino[53a,53b], Y. Sano[105], A. Sansoni[50], C. Santoni[37], H. Santos[128a], I. Santoyo Castillo[151], A. Sapronov[68], J.G. Saraiva[128a,128d], B. Sarrazin[23], O. Sasaki[69], K. Sato[164], E. Sauvan[5], G. Savage[80], P. Savard[161,d], N. Savic[103], C. Sawyer[133], L. Sawyer[82,u], J. Saxon[33], C. Sbarra[22a], A. Sbrizzi[22a,22b], T. Scanlon[81], D.A. Scannicchio[166], J. Schaarschmidt[140], P. Schacht[103], B.M. Schachtner[102], D. Schaefer[32], L. Schaefer[124], R. Schaefer[45], J. Schaeffer[86], S. Schaepe[23], S. Schaetzel[60b], U. Schäfer[86], A.C. Schaffer[119], D. Schaile[102], R.D. Schamberger[150], V.A. Schegelsky[125], D. Scheirich[131], M. Schernau[166], C. Schiavi[53a,53b], S. Schier[139], L.K. Schildgen[23], C. Schillo[51], M. Schioppa[40a,40b], S. Schlenker[32], K.R. Schmidt-Sommerfeld[103], K. Schmieden[32], C. Schmitt[86], S. Schmitt[45], S. Schmitz[86], U. Schnoor[51], L. Schoeffel[138], A. Schoening[60b], B.D. Schoenrock[93], E. Schopf[23], M. Schott[86], J.F.P. Schouwenberg[108], J. Schovancova[32], S. Schramm[52], N. Schuh[86], A. Schulte[86], M.J. Schultens[23], H.-C. Schultz-Coulon[60a], H. Schulz[17], M. Schumacher[51], B.A. Schumm[139], Ph. Schune[138], A. Schwartzman[145], T.A. Schwarz[92], H. Schweiger[87], Ph. Schwemling[138], R. Schwienhorst[93], J. Schwindling[138], A. Sciandra[23], G. Sciolla[25], M. Scornajenghi[40a,40b], F. Scuri[126a,126b], F. Scutti[91], J. Searcy[92], P. Seema[23], S.C. Seidel[107], A. Seiden[139], J.M. Seixas[26a], G. Sekhniaidze[106a], K. Sekhon[92], S.J. Sekula[43], N. Semprini-Cesari[22a,22b], S. Senkin[37], C. Serfon[121], L. Serin[119], L. Serkin[167a,167b], M. Sessa[136a,136b], R. Seuster[172], H. Severini[115], T. Sfiligoj[78], F. Sforza[165], A. Sfyrla[52], E. Shabalina[57], N.W. Shaikh[148a,148b], L.Y. Shan[35a], R. Shang[169], J.T. Shank[24], M. Shapiro[16], P.B. Shatalov[99], K. Shaw[167a,167b], S.M. Shaw[87], A. Shcherbakova[148a,148b], C.Y. Shehu[151], Y. Shen[115], N. Sherafati[31], P. Sherwood[81], L. Shi[153,an], S. Shimizu[70], C.O. Shimmin[179], M. Shimojima[104], I.P.J. Shipsey[122], S. Shirabe[73], M. Shiyakova[68,ao], J. Shlomi[175], A. Shmeleva[98], D. Shoaleh Saadi[97], M.J. Shochet[33], S. Shojaii[94a], D.R. Shope[115], S. Shrestha[113], E. Shulga[100], M.A. Shupe[7], P. Sicho[129], A.M. Sickles[169], P.E. Sidebo[149], E. Sideras Haddad[147c], O. Sidiropoulou[177], A. Sidoti[22a,22b], F. Siegert[47], Dj. Sijacki[14], J. Silva[128a,128d], S.B. Silverstein[148a], V. Simak[130], Lj. Simic[14], S. Simion[119], E. Simioni[86], B. Simmons[81], M. Simon[86], P. Sinervo[161], N.B. Sinev[118], M. Sioli[22a,22b], G. Siragusa[177], I. Siral[92], S.Yu. Sivoklokov[101], J. Sjölin[148a,148b], M.B. Skinner[75], P. Skubic[115], M. Slater[19], T. Slavicek[130], M. Slawinska[42], K. Sliwa[165], R. Slovak[131], V. Smakhtin[175], B.H. Smart[5], J. Smiesko[146a], N. Smirnov[100], S.Yu. Smirnov[100], Y. Smirnov[100], L.N. Smirnova[101,ap], O. Smirnova[84], J.W. Smith[57], M.N.K. Smith[38], R.W. Smith[38], M. Smizanska[75], K. Smolek[130], A.A. Snesarev[98], I.M. Snyder[118], S. Snyder[27], R. Sobie[172,o], F. Socher[47], A. Soffer[155], A. Søgaard[49], D.A. Soh[153], G. Sokhrannyi[78], C.A. Solans Sanchez[32], M. Solar[130], E.Yu. Soldatov[100], U. Soldevila[170], A.A. Solodkov[132], A. Soloshenko[68], O.V. Solovyanov[132], V. Solovyev[125], P. Sommer[51], H. Son[165], A. Sopczak[130], D. Sosa[60b], C.L. Sotiropoulou[126a,126b], R. Soualah[167a,167c], A.M. Soukharev[111,c], D. South[45], B.C. Sowden[80], S. Spagnolo[76a,76b], M. Spalla[126a,126b], M. Spangenberg[173], F. Spanò[80], D. Sperlich[17], F. Spettel[103], T.M. Spieker[60a], R. Spighi[22a], G. Spigo[32], L.A. Spiller[91], M. Spousta[131], R.D. St. Denis[56,*], A. Stabile[94a], R. Stamen[60a], S. Stamm[17], E. Stanecka[42], R.W. Stanek[6], C. Stanescu[136a], M.M. Stanitzki[45], B.S. Stapf[109], S. Stapnes[121], E.A. Starchenko[132], G.H. Stark[33], J. Stark[58], S.H Stark[39], P. Staroba[129], P. Starovoitov[60a], S. Stärz[32], R. Staszewski[42], P. Steinberg[27], B. Stelzer[144], H.J. Stelzer[32], O. Stelzer-Chilton[163a], H. Stenzel[55], G.A. Stewart[56], M.C. Stockton[118], M. Stoebe[90], G. Stoicea[28b], P. Stolte[57], S. Stonjek[103],

JHEP10(2017)129

A.R. Stradling[8], A. Straessner[47], M.E. Stramaglia[18], J. Strandberg[149], S. Strandberg[148a,148b], M. Strauss[115], P. Strizenec[146b], R. Ströhmer[177], D.M. Strom[118], R. Stroynowski[43], A. Strubig[49], S.A. Stucci[27], B. Stugu[15], N.A. Styles[45], D. Su[145], J. Su[127], S. Suchek[60a], Y. Sugaya[120], M. Suk[130], V.V. Sulin[98], DMS Sultan[162a,162b], S. Sultansoy[4c], T. Sumida[71], S. Sun[59], X. Sun[3], K. Suruliz[151], C.J.E. Suster[152], M.R. Sutton[151], S. Suzuki[69], M. Svatos[129], M. Swiatlowski[33], S.P. Swift[2], I. Sykora[146a], T. Sykora[131], D. Ta[51], K. Tackmann[45], J. Taenzer[155], A. Taffard[166], R. Tafirout[163a], E. Tahirovic[79], N. Taiblum[155], H. Takai[27], R. Takashima[72], E.H. Takasugi[103], T. Takeshita[142], Y. Takubo[69], M. Talby[88], A.A. Talyshev[111,c], J. Tanaka[157], M. Tanaka[159], R. Tanaka[119], S. Tanaka[69], R. Tanioka[70], B.B. Tannenwald[113], S. Tapia Araya[34b], S. Tapprogge[86], S. Tarem[154], G.F. Tartarelli[94a], P. Tas[131], M. Tasevsky[129], T. Tashiro[71], E. Tassi[40a,40b], A. Tavares Delgado[128a,128b], Y. Tayalati[137e], A.C. Taylor[107], A.J. Taylor[49], G.N. Taylor[91], P.T.E. Taylor[91], W. Taylor[163b], P. Teixeira-Dias[80], D. Temple[144], H. Ten Kate[32], P.K. Teng[153], J.J. Teoh[120], F. Tepel[178], S. Terada[69], K. Terashi[157], J. Terron[85], S. Terzo[13], M. Testa[50], R.J. Teuscher[161,o], T. Theveneaux-Pelzer[88], F. Thiele[39], J.P. Thomas[19], J. Thomas-Wilsker[80], P.D. Thompson[19], A.S. Thompson[56], L.A. Thomsen[179], E. Thomson[124], M.J. Tibbetts[16], R.E. Ticse Torres[88], V.O. Tikhomirov[98,aq], Yu.A. Tikhonov[111,c], S. Timoshenko[100], P. Tipton[179], S. Tisserant[88], K. Todome[159], S. Todorova-Nova[5], S. Todt[47], J. Tojo[73], S. Tokár[146a], K. Tokushuku[69], E. Tolley[59], L. Tomlinson[87], M. Tomoto[105], L. Tompkins[145,ar], K. Toms[107], B. Tong[59], P. Tornambe[51], E. Torrence[118], H. Torres[47], E. Torró Pastor[140], J. Toth[88,as], F. Touchard[88], D.R. Tovey[141], C.J. Treado[112], T. Trefzger[177], F. Tresoldi[151], A. Tricoli[27], I.M. Trigger[163a], S. Trincaz-Duvoid[83], M.F. Tripiana[13], W. Trischuk[161], B. Trocmé[58], A. Trofymov[45], C. Troncon[94a], M. Trottier-McDonald[16], M. Trovatelli[172], L. Truong[147b], M. Trzebinski[42], A. Trzupek[42], K.W. Tsang[62a], J.C-L. Tseng[122], P.V. Tsiareshka[95], G. Tsipolitis[10], N. Tsirintanis[9], S. Tsiskaridze[13], V. Tsiskaridze[51], E.G. Tskhadadze[54a], K.M. Tsui[62a], I.I. Tsukerman[99], V. Tsulaia[16], S. Tsuno[69], D. Tsybychev[150], Y. Tu[62b], A. Tudorache[28b], V. Tudorache[28b], T.T. Tulbure[28a], A.N. Tuna[59], S.A. Tupputi[22a,22b], S. Turchikhin[68], D. Turgeman[175], I. Turk Cakir[4b,at], R. Turra[94a], P.M. Tuts[38], G. Ucchielli[22a,22b], I. Ueda[69], M. Ughetto[148a,148b], F. Ukegawa[164], G. Unal[32], A. Undrus[27], G. Unel[166], F.C. Ungaro[91], Y. Unno[69], C. Unverdorben[102], J. Urban[146b], P. Urquijo[91], P. Urrejola[86], G. Usai[8], J. Usui[69], L. Vacavant[88], V. Vacek[130], B. Vachon[90], K.O.H. Vadla[121], A. Vaidya[81], C. Valderanis[102], E. Valdes Santurio[148a,148b], M. Valente[52], S. Valentinetti[22a,22b], A. Valero[170], L. Valéry[13], S. Valkar[131], A. Vallier[5], J.A. Valls Ferrer[170], W. Van Den Wollenberg[109], H. van der Graaf[109], P. van Gemmeren[6], J. Van Nieuwkoop[144], I. van Vulpen[109], M.C. van Woerden[109], M. Vanadia[135a,135b], W. Vandelli[32], A. Vaniachine[160], P. Vankov[109], G. Vardanyan[180], R. Vari[134a], E.W. Varnes[7], C. Varni[53a,53b], T. Varol[43], D. Varouchas[119], A. Vartapetian[8], K.E. Varvell[152], J.G. Vasquez[179], G.A. Vasquez[34b], F. Vazeille[37], T. Vazquez Schroeder[90], J. Veatch[57], V. Veeraraghavan[7], L.M. Veloce[161], F. Veloso[128a,128c], S. Veneziano[134a], A. Ventura[76a,76b], M. Venturi[172], N. Venturi[32], A. Venturini[25], V. Vercesi[123a], M. Verducci[136a,136b], W. Verkerke[109], A.T. Vermeulen[109], J.C. Vermeulen[109], M.C. Vetterli[144,d], N. Viaux Maira[34b], O. Viazlo[84], I. Vichou[169,*], T. Vickey[141], O.E. Vickey Boeriu[141], G.H.A. Viehhauser[122], S. Viel[16], L. Vigani[122], M. Villa[22a,22b], M. Villaplana Perez[94a,94b], E. Vilucchi[50], M.G. Vincter[31], V.B. Vinogradov[68], A. Vishwakarma[45], C. Vittori[22a,22b], I. Vivarelli[151], S. Vlachos[10], M. Vogel[178], P. Vokac[130], G. Volpi[13], H. von der Schmitt[103], E. von Toerne[23], V. Vorobel[131], K. Vorobev[100], M. Vos[170], R. Voss[32], J.H. Vossebeld[77], N. Vranjes[14], M. Vranjes Milosavljevic[14], V. Vrba[130], M. Vreeswijk[109], R. Vuillermet[32], I. Vukotic[33], P. Wagner[23], W. Wagner[178], J. Wagner-Kuhr[102], H. Wahlberg[74], S. Wahrmund[47], J. Walder[75], R. Walker[102], W. Walkowiak[143], V. Wallangen[148a,148b], C. Wang[35b], C. Wang[36b,au], F. Wang[176], H. Wang[16], H. Wang[3],

JHEP10(2017)129

J. Wang[45], J. Wang[152], Q. Wang[115], R. Wang[6], S.M. Wang[153], T. Wang[38], W. Wang[153,av], W. Wang[36a], Z. Wang[36c], C. Wanotayaroj[118], A. Warburton[90], C.P. Ward[30], D.R. Wardrope[81], A. Washbrook[49], P.M. Watkins[19], A.T. Watson[19], M.F. Watson[19], G. Watts[140], S. Watts[87], B.M. Waugh[81], A.F. Webb[11], S. Webb[86], M.S. Weber[18], S.W. Weber[177], S.A. Weber[31], J.S. Webster[6], A.R. Weidberg[122], B. Weinert[64], J. Weingarten[57], M. Weirich[86], C. Weiser[51], H. Weits[109], P.S. Wells[32], T. Wenaus[27], T. Wengler[32], S. Wenig[32], N. Wermes[23], M.D. Werner[67], P. Werner[32], M. Wessels[60a], T.D. Weston[18], K. Whalen[118], N.L. Whallon[140], A.M. Wharton[75], A.S. White[92], A. White[8], M.J. White[1], R. White[34b], D. Whiteson[166], B.W. Whitmore[75], F.J. Wickens[133], W. Wiedenmann[176], M. Wielers[133], C. Wiglesworth[39], L.A.M. Wiik-Fuchs[51], A. Wildauer[103], F. Wilk[87], H.G. Wilkens[32], H.H. Williams[124], S. Williams[109], C. Willis[93], S. Willocq[89], J.A. Wilson[19], I. Wingerter-Seez[5], E. Winkels[151], F. Winklmeier[118], O.J. Winston[151], B.T. Winter[23], M. Wittgen[145], M. Wobisch[82,u], T.M.H. Wolf[109], R. Wolff[88], M.W. Wolter[42], H. Wolters[128a,128c], V.W.S. Wong[171], S.D. Worm[19], B.K. Wosiek[42], J. Wotschack[32], K.W. Wozniak[42], M. Wu[33], S.L. Wu[176], X. Wu[52], Y. Wu[92], T.R. Wyatt[87], B.M. Wynne[49], S. Xella[39], Z. Xi[92], L. Xia[35c], D. Xu[35a], L. Xu[27], T. Xu[138], B. Yabsley[152], S. Yacoob[147a], D. Yamaguchi[159], Y. Yamaguchi[159], A. Yamamoto[69], S. Yamamoto[157], T. Yamanaka[157], F. Yamane[70], M. Yamatani[157], Y. Yamazaki[70], Z. Yan[24], H. Yang[36c], H. Yang[16], Y. Yang[153], Z. Yang[15], W-M. Yao[16], Y.C. Yap[83], Y. Yasu[69], E. Yatsenko[5], K.H. Yau Wong[23], J. Ye[43], S. Ye[27], I. Yeletskikh[68], E. Yigitbasi[24], E. Yildirim[86], K. Yorita[174], K. Yoshihara[124], C. Young[145], C.J.S. Young[32], J. Yu[8], J. Yu[67], S.P.Y. Yuen[23], I. Yusuff[30,aw], B. Zabinski[42], G. Zacharis[10], R. Zaidan[13], A.M. Zaitsev[132,ak], N. Zakharchuk[45], J. Zalieckas[15], A. Zaman[150], S. Zambito[59], D. Zanzi[91], C. Zeitnitz[178], G. Zemaityte[122], A. Zemla[41a], J.C. Zeng[169], Q. Zeng[145], O. Zenin[132], T. Ženiš[146a], D. Zerwas[119], D. Zhang[92], F. Zhang[176], G. Zhang[36a,ax], H. Zhang[119], J. Zhang[6], L. Zhang[51], L. Zhang[36a], M. Zhang[169], P. Zhang[35b], R. Zhang[23], R. Zhang[36a,au], X. Zhang[36b], Y. Zhang[35a], Z. Zhang[119], X. Zhao[43], Y. Zhao[36b,ay], Z. Zhao[36a], A. Zhemchugov[68], B. Zhou[92], C. Zhou[176], L. Zhou[43], M. Zhou[35a], M. Zhou[150], N. Zhou[35c], C.G. Zhu[36b], H. Zhu[35a], J. Zhu[92], Y. Zhu[36a], X. Zhuang[35a], K. Zhukov[98], A. Zibell[177], D. Zieminska[64], N.I. Zimine[68], C. Zimmermann[86], S. Zimmermann[51], Z. Zinonos[103], M. Zinser[86], M. Ziolkowski[143], L. Živković[14], G. Zobernig[176], A. Zoccoli[22a,22b], R. Zou[33], M. zur Nedden[17], L. Zwalinski[32].

[1] *Department of Physics, University of Adelaide, Adelaide, Australia*
[2] *Physics Department, SUNY Albany, Albany NY, United States of America*
[3] *Department of Physics, University of Alberta, Edmonton AB, Canada*
[4] [(a)] *Department of Physics, Ankara University, Ankara;* [(b)] *Istanbul Aydin University, Istanbul;* [(c)] *Division of Physics, TOBB University of Economics and Technology, Ankara, Turkey*
[5] *LAPP, CNRS/IN2P3 and Université Savoie Mont Blanc, Annecy-le-Vieux, France*
[6] *High Energy Physics Division, Argonne National Laboratory, Argonne IL, United States of America*
[7] *Department of Physics, University of Arizona, Tucson AZ, United States of America*
[8] *Department of Physics, The University of Texas at Arlington, Arlington TX, United States of America*
[9] *Physics Department, National and Kapodistrian University of Athens, Athens, Greece*
[10] *Physics Department, National Technical University of Athens, Zografou, Greece*
[11] *Department of Physics, The University of Texas at Austin, Austin TX, United States of America*
[12] *Institute of Physics, Azerbaijan Academy of Sciences, Baku, Azerbaijan*
[13] *Institut de Física d'Altes Energies (IFAE), The Barcelona Institute of Science and Technology, Barcelona, Spain*
[14] *Institute of Physics, University of Belgrade, Belgrade, Serbia*
[15] *Department for Physics and Technology, University of Bergen, Bergen, Norway*

JHEP10(2017)129

[16] Physics Division, Lawrence Berkeley National Laboratory and University of California, Berkeley CA, United States of America
[17] Department of Physics, Humboldt University, Berlin, Germany
[18] Albert Einstein Center for Fundamental Physics and Laboratory for High Energy Physics, University of Bern, Bern, Switzerland
[19] School of Physics and Astronomy, University of Birmingham, Birmingham, United Kingdom
[20] [(a)] Department of Physics, Bogazici University, Istanbul; [(b)] Department of Physics Engineering, Gaziantep University, Gaziantep; [(d)] Istanbul Bilgi University, Faculty of Engineering and Natural Sciences, Istanbul; [(e)] Bahcesehir University, Faculty of Engineering and Natural Sciences, Istanbul, Turkey
[21] Centro de Investigaciones, Universidad Antonio Narino, Bogota, Colombia
[22] [(a)] INFN Sezione di Bologna; [(b)] Dipartimento di Fisica e Astronomia, Università di Bologna, Bologna, Italy
[23] Physikalisches Institut, University of Bonn, Bonn, Germany
[24] Department of Physics, Boston University, Boston MA, United States of America
[25] Department of Physics, Brandeis University, Waltham MA, United States of America
[26] [(a)] Universidade Federal do Rio De Janeiro COPPE/EE/IF, Rio de Janeiro; [(b)] Electrical Circuits Department, Federal University of Juiz de Fora (UFJF), Juiz de Fora; [(c)] Federal University of Sao Joao del Rei (UFSJ), Sao Joao del Rei; [(d)] Instituto de Fisica, Universidade de Sao Paulo, Sao Paulo, Brazil
[27] Physics Department, Brookhaven National Laboratory, Upton NY, United States of America
[28] [(a)] Transilvania University of Brasov, Brasov; [(b)] Horia Hulubei National Institute of Physics and Nuclear Engineering, Bucharest; [(c)] Department of Physics, Alexandru Ioan Cuza University of Iasi, Iasi; [(d)] National Institute for Research and Development of Isotopic and Molecular Technologies, Physics Department, Cluj Napoca; [(e)] University Politehnica Bucharest, Bucharest; [(f)] West University in Timisoara, Timisoara, Romania
[29] Departamento de Física, Universidad de Buenos Aires, Buenos Aires, Argentina
[30] Cavendish Laboratory, University of Cambridge, Cambridge, United Kingdom
[31] Department of Physics, Carleton University, Ottawa ON, Canada
[32] CERN, Geneva, Switzerland
[33] Enrico Fermi Institute, University of Chicago, Chicago IL, United States of America
[34] [(a)] Departamento de Física, Pontificia Universidad Católica de Chile, Santiago; [(b)] Departamento de Física, Universidad Técnica Federico Santa María, Valparaíso, Chile
[35] [(a)] Institute of High Energy Physics, Chinese Academy of Sciences, Beijing; [(b)] Department of Physics, Nanjing University, Jiangsu; [(c)] Physics Department, Tsinghua University, Beijing 100084, China
[36] [(a)] Department of Modern Physics and State Key Laboratory of Particle Detection and Electronics, University of Science and Technology of China, Anhui; [(b)] School of Physics, Shandong University, Shandong; [(c)] Department of Physics and Astronomy, Key Laboratory for Particle Physics, Astrophysics and Cosmology, Ministry of Education; Shanghai Key Laboratory for Particle Physics and Cosmology, Shanghai Jiao Tong University, Shanghai(also at PKU-CHEP), China
[37] Université Clermont Auvergne, CNRS/IN2P3, LPC, Clermont-Ferrand, France
[38] Nevis Laboratory, Columbia University, Irvington NY, United States of America
[39] Niels Bohr Institute, University of Copenhagen, Kobenhavn, Denmark
[40] [(a)] INFN Gruppo Collegato di Cosenza, Laboratori Nazionali di Frascati; [(b)] Dipartimento di Fisica, Università della Calabria, Rende, Italy
[41] [(a)] AGH University of Science and Technology, Faculty of Physics and Applied Computer Science, Krakow; [(b)] Marian Smoluchowski Institute of Physics, Jagiellonian University, Krakow, Poland
[42] Institute of Nuclear Physics Polish Academy of Sciences, Krakow, Poland
[43] Physics Department, Southern Methodist University, Dallas TX, United States of America
[44] Physics Department, University of Texas at Dallas, Richardson TX, United States of America
[45] DESY, Hamburg and Zeuthen, Germany
[46] Lehrstuhl für Experimentelle Physik IV, Technische Universität Dortmund, Dortmund, Germany

JHEP10(2017)129

[47] Institut für Kern- und Teilchenphysik, Technische Universität Dresden, Dresden, Germany
[48] Department of Physics, Duke University, Durham NC, United States of America
[49] SUPA - School of Physics and Astronomy, University of Edinburgh, Edinburgh, United Kingdom
[50] INFN e Laboratori Nazionali di Frascati, Frascati, Italy
[51] Fakultät für Mathematik und Physik, Albert-Ludwigs-Universität, Freiburg, Germany
[52] Departement de Physique Nucleaire et Corpusculaire, Université de Genève, Geneva, Switzerland
[53] [(a)] INFN Sezione di Genova; [(b)] Dipartimento di Fisica, Università di Genova, Genova, Italy
[54] [(a)] E. Andronikashvili Institute of Physics, Iv. Javakhishvili Tbilisi State University, Tbilisi; [(b)] High Energy Physics Institute, Tbilisi State University, Tbilisi, Georgia
[55] II Physikalisches Institut, Justus-Liebig-Universität Giessen, Giessen, Germany
[56] SUPA - School of Physics and Astronomy, University of Glasgow, Glasgow, United Kingdom
[57] II Physikalisches Institut, Georg-August-Universität, Göttingen, Germany
[58] Laboratoire de Physique Subatomique et de Cosmologie, Université Grenoble-Alpes, CNRS/IN2P3, Grenoble, France
[59] Laboratory for Particle Physics and Cosmology, Harvard University, Cambridge MA, United States of America
[60] [(a)] Kirchhoff-Institut für Physik, Ruprecht-Karls-Universität Heidelberg, Heidelberg; [(b)] Physikalisches Institut, Ruprecht-Karls-Universität Heidelberg, Heidelberg, Germany
[61] Faculty of Applied Information Science, Hiroshima Institute of Technology, Hiroshima, Japan
[62] [(a)] Department of Physics, The Chinese University of Hong Kong, Shatin, N.T., Hong Kong; [(b)] Department of Physics, The University of Hong Kong, Hong Kong; [(c)] Department of Physics and Institute for Advanced Study, The Hong Kong University of Science and Technology, Clear Water Bay, Kowloon, Hong Kong, China
[63] Department of Physics, National Tsing Hua University, Taiwan
[64] Department of Physics, Indiana University, Bloomington IN, United States of America
[65] Institut für Astro- und Teilchenphysik, Leopold-Franzens-Universität, Innsbruck, Austria
[66] University of Iowa, Iowa City IA, United States of America
[67] Department of Physics and Astronomy, Iowa State University, Ames IA, United States of America
[68] Joint Institute for Nuclear Research, JINR Dubna, Dubna, Russia
[69] KEK, High Energy Accelerator Research Organization, Tsukuba, Japan
[70] Graduate School of Science, Kobe University, Kobe, Japan
[71] Faculty of Science, Kyoto University, Kyoto, Japan
[72] Kyoto University of Education, Kyoto, Japan
[73] Research Center for Advanced Particle Physics and Department of Physics, Kyushu University, Fukuoka, Japan
[74] Instituto de Física La Plata, Universidad Nacional de La Plata and CONICET, La Plata, Argentina
[75] Physics Department, Lancaster University, Lancaster, United Kingdom
[76] [(a)] INFN Sezione di Lecce; [(b)] Dipartimento di Matematica e Fisica, Università del Salento, Lecce, Italy
[77] Oliver Lodge Laboratory, University of Liverpool, Liverpool, United Kingdom
[78] Department of Experimental Particle Physics, Jožef Stefan Institute and Department of Physics, University of Ljubljana, Ljubljana, Slovenia
[79] School of Physics and Astronomy, Queen Mary University of London, London, United Kingdom
[80] Department of Physics, Royal Holloway University of London, Surrey, United Kingdom
[81] Department of Physics and Astronomy, University College London, London, United Kingdom
[82] Louisiana Tech University, Ruston LA, United States of America
[83] Laboratoire de Physique Nucléaire et de Hautes Energies, UPMC and Université Paris-Diderot and CNRS/IN2P3, Paris, France
[84] Fysiska institutionen, Lunds universitet, Lund, Sweden
[85] Departamento de Fisica Teorica C-15, Universidad Autonoma de Madrid, Madrid, Spain
[86] Institut für Physik, Universität Mainz, Mainz, Germany
[87] School of Physics and Astronomy, University of Manchester, Manchester, United Kingdom
[88] CPPM, Aix-Marseille Université and CNRS/IN2P3, Marseille, France

JHEP10(2017)129

[89] Department of Physics, University of Massachusetts, Amherst MA, United States of America
[90] Department of Physics, McGill University, Montreal QC, Canada
[91] School of Physics, University of Melbourne, Victoria, Australia
[92] Department of Physics, The University of Michigan, Ann Arbor MI, United States of America
[93] Department of Physics and Astronomy, Michigan State University, East Lansing MI, United States of America
[94] [(a)] INFN Sezione di Milano; [(b)] Dipartimento di Fisica, Università di Milano, Milano, Italy
[95] B.I. Stepanov Institute of Physics, National Academy of Sciences of Belarus, Minsk, Republic of Belarus
[96] Research Institute for Nuclear Problems of Byelorussian State University, Minsk, Republic of Belarus
[97] Group of Particle Physics, University of Montreal, Montreal QC, Canada
[98] P.N. Lebedev Physical Institute of the Russian Academy of Sciences, Moscow, Russia
[99] Institute for Theoretical and Experimental Physics (ITEP), Moscow, Russia
[100] National Research Nuclear University MEPhI, Moscow, Russia
[101] D.V. Skobeltsyn Institute of Nuclear Physics, M.V. Lomonosov Moscow State University, Moscow, Russia
[102] Fakultät für Physik, Ludwig-Maximilians-Universität München, München, Germany
[103] Max-Planck-Institut für Physik (Werner-Heisenberg-Institut), München, Germany
[104] Nagasaki Institute of Applied Science, Nagasaki, Japan
[105] Graduate School of Science and Kobayashi-Maskawa Institute, Nagoya University, Nagoya, Japan
[106] [(a)] INFN Sezione di Napoli; [(b)] Dipartimento di Fisica, Università di Napoli, Napoli, Italy
[107] Department of Physics and Astronomy, University of New Mexico, Albuquerque NM, United States of America
[108] Institute for Mathematics, Astrophysics and Particle Physics, Radboud University Nijmegen/Nikhef, Nijmegen, Netherlands
[109] Nikhef National Institute for Subatomic Physics and University of Amsterdam, Amsterdam, Netherlands
[110] Department of Physics, Northern Illinois University, DeKalb IL, United States of America
[111] Budker Institute of Nuclear Physics, SB RAS, Novosibirsk, Russia
[112] Department of Physics, New York University, New York NY, United States of America
[113] Ohio State University, Columbus OH, United States of America
[114] Faculty of Science, Okayama University, Okayama, Japan
[115] Homer L. Dodge Department of Physics and Astronomy, University of Oklahoma, Norman OK, United States of America
[116] Department of Physics, Oklahoma State University, Stillwater OK, United States of America
[117] Palacký University, RCPTM, Olomouc, Czech Republic
[118] Center for High Energy Physics, University of Oregon, Eugene OR, United States of America
[119] LAL, Univ. Paris-Sud, CNRS/IN2P3, Université Paris-Saclay, Orsay, France
[120] Graduate School of Science, Osaka University, Osaka, Japan
[121] Department of Physics, University of Oslo, Oslo, Norway
[122] Department of Physics, Oxford University, Oxford, United Kingdom
[123] [(a)] INFN Sezione di Pavia; [(b)] Dipartimento di Fisica, Università di Pavia, Pavia, Italy
[124] Department of Physics, University of Pennsylvania, Philadelphia PA, United States of America
[125] National Research Centre "Kurchatov Institute" B.P.Konstantinov Petersburg Nuclear Physics Institute, St. Petersburg, Russia
[126] [(a)] INFN Sezione di Pisa; [(b)] Dipartimento di Fisica E. Fermi, Università di Pisa, Pisa, Italy
[127] Department of Physics and Astronomy, University of Pittsburgh, Pittsburgh PA, United States of America
[128] [(a)] Laboratório de Instrumentação e Física Experimental de Partículas - LIP, Lisboa; [(b)] Faculdade de Ciências, Universidade de Lisboa, Lisboa; [(c)] Department of Physics, University of Coimbra, Coimbra; [(d)] Centro de Física Nuclear da Universidade de Lisboa, Lisboa; [(e)] Departamento de Fisica, Universidade do Minho, Braga; [(f)] Departamento de Fisica Teorica y del Cosmos and CAFPE, Universidad de Granada, Granada; [(g)] Dep Fisica and CEFITEC of Faculdade de Ciencias e Tecnologia, Universidade Nova de Lisboa, Caparica, Portugal

JHEP10(2017)129

[129] Institute of Physics, Academy of Sciences of the Czech Republic, Praha, Czech Republic
[130] Czech Technical University in Prague, Praha, Czech Republic
[131] Charles University, Faculty of Mathematics and Physics, Prague, Czech Republic
[132] State Research Center Institute for High Energy Physics (Protvino), NRC KI, Russia
[133] Particle Physics Department, Rutherford Appleton Laboratory, Didcot, United Kingdom
[134] [(a)] INFN Sezione di Roma; [(b)] Dipartimento di Fisica, Sapienza Università di Roma, Roma, Italy
[135] [(a)] INFN Sezione di Roma Tor Vergata; [(b)] Dipartimento di Fisica, Università di Roma Tor Vergata, Roma, Italy
[136] [(a)] INFN Sezione di Roma Tre; [(b)] Dipartimento di Matematica e Fisica, Università Roma Tre, Roma, Italy
[137] [(a)] Faculté des Sciences Ain Chock, Réseau Universitaire de Physique des Hautes Energies - Université Hassan II, Casablanca; [(b)] Centre National de l'Energie des Sciences Techniques Nucleaires, Rabat; [(c)] Faculté des Sciences Semlalia, Université Cadi Ayyad, LPHEA-Marrakech; [(d)] Faculté des Sciences, Université Mohamed Premier and LPTPM, Oujda; [(e)] Faculté des sciences, Université Mohammed V, Rabat, Morocco
[138] DSM/IRFU (Institut de Recherches sur les Lois Fondamentales de l'Univers), CEA Saclay (Commissariat à l'Energie Atomique et aux Energies Alternatives), Gif-sur-Yvette, France
[139] Santa Cruz Institute for Particle Physics, University of California Santa Cruz, Santa Cruz CA, United States of America
[140] Department of Physics, University of Washington, Seattle WA, United States of America
[141] Department of Physics and Astronomy, University of Sheffield, Sheffield, United Kingdom
[142] Department of Physics, Shinshu University, Nagano, Japan
[143] Department Physik, Universität Siegen, Siegen, Germany
[144] Department of Physics, Simon Fraser University, Burnaby BC, Canada
[145] SLAC National Accelerator Laboratory, Stanford CA, United States of America
[146] [(a)] Faculty of Mathematics, Physics & Informatics, Comenius University, Bratislava; [(b)] Department of Subnuclear Physics, Institute of Experimental Physics of the Slovak Academy of Sciences, Kosice, Slovak Republic
[147] [(a)] Department of Physics, University of Cape Town, Cape Town; [(b)] Department of Physics, University of Johannesburg, Johannesburg; [(c)] School of Physics, University of the Witwatersrand, Johannesburg, South Africa
[148] [(a)] Department of Physics, Stockholm University; [(b)] The Oskar Klein Centre, Stockholm, Sweden
[149] Physics Department, Royal Institute of Technology, Stockholm, Sweden
[150] Departments of Physics & Astronomy and Chemistry, Stony Brook University, Stony Brook NY, United States of America
[151] Department of Physics and Astronomy, University of Sussex, Brighton, United Kingdom
[152] School of Physics, University of Sydney, Sydney, Australia
[153] Institute of Physics, Academia Sinica, Taipei, Taiwan
[154] Department of Physics, Technion: Israel Institute of Technology, Haifa, Israel
[155] Raymond and Beverly Sackler School of Physics and Astronomy, Tel Aviv University, Tel Aviv, Israel
[156] Department of Physics, Aristotle University of Thessaloniki, Thessaloniki, Greece
[157] International Center for Elementary Particle Physics and Department of Physics, The University of Tokyo, Tokyo, Japan
[158] Graduate School of Science and Technology, Tokyo Metropolitan University, Tokyo, Japan
[159] Department of Physics, Tokyo Institute of Technology, Tokyo, Japan
[160] Tomsk State University, Tomsk, Russia
[161] Department of Physics, University of Toronto, Toronto ON, Canada
[162] [(a)] INFN-TIFPA; [(b)] University of Trento, Trento, Italy
[163] [(a)] TRIUMF, Vancouver BC; [(b)] Department of Physics and Astronomy, York University, Toronto ON, Canada
[164] Faculty of Pure and Applied Sciences, and Center for Integrated Research in Fundamental Science and Engineering, University of Tsukuba, Tsukuba, Japan

JHEP10(2017)129

[165] Department of Physics and Astronomy, Tufts University, Medford MA, United States of America
[166] Department of Physics and Astronomy, University of California Irvine, Irvine CA, United States of America
[167] [(a)] INFN Gruppo Collegato di Udine, Sezione di Trieste, Udine; [(b)] ICTP, Trieste; [(c)] Dipartimento di Chimica, Fisica e Ambiente, Università di Udine, Udine, Italy
[168] Department of Physics and Astronomy, University of Uppsala, Uppsala, Sweden
[169] Department of Physics, University of Illinois, Urbana IL, United States of America
[170] Instituto de Fisica Corpuscular (IFIC), Centro Mixto Universidad de Valencia - CSIC, Spain
[171] Department of Physics, University of British Columbia, Vancouver BC, Canada
[172] Department of Physics and Astronomy, University of Victoria, Victoria BC, Canada
[173] Department of Physics, University of Warwick, Coventry, United Kingdom
[174] Waseda University, Tokyo, Japan
[175] Department of Particle Physics, The Weizmann Institute of Science, Rehovot, Israel
[176] Department of Physics, University of Wisconsin, Madison WI, United States of America
[177] Fakultät für Physik und Astronomie, Julius-Maximilians-Universität, Würzburg, Germany
[178] Fakultät für Mathematik und Naturwissenschaften, Fachgruppe Physik, Bergische Universität Wuppertal, Wuppertal, Germany
[179] Department of Physics, Yale University, New Haven CT, United States of America
[180] Yerevan Physics Institute, Yerevan, Armenia
[181] Centre de Calcul de l'Institut National de Physique Nucléaire et de Physique des Particules (IN2P3), Villeurbanne, France
[182] Academia Sinica Grid Computing, Institute of Physics, Academia Sinica, Taipei, Taiwan

[a] Also at Department of Physics, King's College London, London, United Kingdom
[b] Also at Institute of Physics, Azerbaijan Academy of Sciences, Baku, Azerbaijan
[c] Also at Novosibirsk State University, Novosibirsk, Russia
[d] Also at TRIUMF, Vancouver BC, Canada
[e] Also at Department of Physics & Astronomy, University of Louisville, Louisville, KY, United States of America
[f] Also at Physics Department, An-Najah National University, Nablus, Palestine
[g] Also at Department of Physics, California State University, Fresno CA, United States of America
[h] Also at Department of Physics, University of Fribourg, Fribourg, Switzerland
[i] Also at II Physikalisches Institut, Georg-August-Universität, Göttingen, Germany
[j] Also at Departament de Fisica de la Universitat Autonoma de Barcelona, Barcelona, Spain
[k] Also at Departamento de Fisica e Astronomia, Faculdade de Ciencias, Universidade do Porto, Portugal
[l] Also at Tomsk State University, Tomsk, Russia
[m] Also at The Collaborative Innovation Center of Quantum Matter (CICQM), Beijing, China
[n] Also at Universita di Napoli Parthenope, Napoli, Italy
[o] Also at Institute of Particle Physics (IPP), Canada
[p] Also at Horia Hulubei National Institute of Physics and Nuclear Engineering, Bucharest, Romania
[q] Also at Department of Physics, St. Petersburg State Polytechnical University, St. Petersburg, Russia
[r] Also at Borough of Manhattan Community College, City University of New York, New York City, United States of America
[s] Also at Department of Financial and Management Engineering, University of the Aegean, Chios, Greece
[t] Also at Centre for High Performance Computing, CSIR Campus, Rosebank, Cape Town, South Africa
[u] Also at Louisiana Tech University, Ruston LA, United States of America
[v] Also at Institucio Catalana de Recerca i Estudis Avancats, ICREA, Barcelona, Spain
[w] Also at Graduate School of Science, Osaka University, Osaka, Japan
[x] Also at Fakultät für Mathematik und Physik, Albert-Ludwigs-Universität, Freiburg, Germany

JHEP10(2017)129

[y] Also at Institute for Mathematics, Astrophysics and Particle Physics, Radboud University Nijmegen/Nikhef, Nijmegen, Netherlands
[z] Also at Department of Physics, The University of Texas at Austin, Austin TX, United States of America
[aa] Also at Institute of Theoretical Physics, Ilia State University, Tbilisi, Georgia
[ab] Also at CERN, Geneva, Switzerland
[ac] Also at Georgian Technical University (GTU),Tbilisi, Georgia
[ad] Also at Ochadai Academic Production, Ochanomizu University, Tokyo, Japan
[ae] Also at Manhattan College, New York NY, United States of America
[af] Also at Departamento de Física, Pontificia Universidad Católica de Chile, Santiago, Chile
[ag] Also at Department of Physics, The University of Michigan, Ann Arbor MI, United States of America
[ah] Also at The City College of New York, New York NY, United States of America
[ai] Also at Departamento de Fisica Teorica y del Cosmos and CAFPE, Universidad de Granada, Granada, Portugal
[aj] Also at Department of Physics, California State University, Sacramento CA, United States of America
[ak] Also at Moscow Institute of Physics and Technology State University, Dolgoprudny, Russia
[al] Also at Departement de Physique Nucleaire et Corpusculaire, Université de Genève, Geneva, Switzerland
[am] Also at Institut de Física d'Altes Energies (IFAE), The Barcelona Institute of Science and Technology, Barcelona, Spain
[an] Also at School of Physics, Sun Yat-sen University, Guangzhou, China
[ao] Also at Institute for Nuclear Research and Nuclear Energy (INRNE) of the Bulgarian Academy of Sciences, Sofia, Bulgaria
[ap] Also at Faculty of Physics, M.V.Lomonosov Moscow State University, Moscow, Russia
[aq] Also at National Research Nuclear University MEPhI, Moscow, Russia
[ar] Also at Department of Physics, Stanford University, Stanford CA, United States of America
[as] Also at Institute for Particle and Nuclear Physics, Wigner Research Centre for Physics, Budapest, Hungary
[at] Also at Giresun University, Faculty of Engineering, Turkey
[au] Also at CPPM, Aix-Marseille Université and CNRS/IN2P3, Marseille, France
[av] Also at Department of Physics, Nanjing University, Jiangsu, China
[aw] Also at University of Malaya, Department of Physics, Kuala Lumpur, Malaysia
[ax] Also at Institute of Physics, Academia Sinica, Taipei, Taiwan
[ay] Also at LAL, Univ. Paris-Sud, CNRS/IN2P3, Université Paris-Saclay, Orsay, France
[*] Deceased

JHEP10(2017)129